FLUID DYNAMICS STUDY ON THE EFFECT OF THE MAXIMUM VALVE LIFT TO THE FLOW VELOCITY AT THE INTAKE VALVE OF GASOLINE ENGINE

MUHAMAD RAZI BIN SAMSUDIN

FACULTY OF ENGINEERING
UNIVERSITY OF MALAYA
KUALA LUMPUR

2019

FLUID DYNAMICS STUDY ON THE EFFECT OF THE MAXIMUM VALVE LIFT TO THE FLOW VELOCITY AT THE INTAKE VALVE OF GASOLINE ENGINE

MUHAMAD RAZI BIN SAMSUDIN

RESEARCH PROJECT SUBMITTED IN PARTIAL FULFILMENT OF THE REQUIREMENTS FOR THE DEGREE OF MASTER OF MECHANICAL ENGINEERING

FACULTY OF ENGINEERING
UNIVERSITY OF MALAYA
KUALA LUMPUR

2019

UNIVERSITY OF MALAYA

ORIGINAL LITERARY WORK DECLARATION

Name of Candidate: Muhamad Razi Bin Samsudin

Matric No: KQK 170024

Name of Degree: Master of Mechanical Engineering

Fluid Dynamics Study on The Effect of The Maximum Valve Lift to The Flow Velocity at The Intake Valve of Gasoline Engine ("this Work"):

Field of Study: Fluid Flow

I do solemnly and sincerely declare that:

(1) I am the sole author/writer of this Work;
(2) This Work is original;
(3) Any use of any work in which copyright exists was done by way of fair dealing and for permitted purposes and any excerpt or extract from, or reference to or reproduction of any copyright work has been disclosed expressly and sufficiently and the title of the Work and its authorship have been acknowledged in this Work;
(4) I do not have any actual knowledge nor do I ought reasonably to know that the making of this work constitutes an infringement of any copyright work;
(5) I hereby assign all and every rights in the copyright to this Work to the University of Malaya ("UM"), who henceforth shall be owner of the copyright in this Work and that any reproduction or use in any form or by any means whatsoever is prohibited without the written consent of UM having been first had and obtained;
(6) I am fully aware that if in the course of making this Work I have infringed any copyright whether intentionally or otherwise, I may be subject to legal action or any other action as may be determined by UM.

Candidate's Signature Date:

Subscribed and solemnly declared before,

Witness's Signature Date:

Name:

Designation:

FLUID DYNAMICS STUDY ON THE EFFECT OF THE MAXIMUM VALVE LIFT TO THE FLOW VELOCITY AT THE INTAKE VALVE OF GASOLINE ENGINE

ABSTRACT

Intake valve lift height value plays a very important role in ensuring the power and performance of the ICE. Low lift valve will restrict the airflow into the engine cylinder. Less amount of air-fuel mixture will cause low energy combustion of ICE. Using high profile cam can increase airflow into the combustion chamber. However, increasing the valve lift beyond the maximum valve lift value will not give any additional flow of fluid into the combustion chamber. Higher lift often requires longer camshaft duration and increase valve train work, which can affect the performance and durability of the engine. Determining the optimum valve lift value is important to maintain the effectiveness and performance of the gasoline engine. Fluid flow studies around an intake valve in ICE are difficult to experiment with due to the position and size of small components moving at high speeds in the engine. Therefore, the use of CFD is the best method for this project. The analysis was conducted to determine the highest valve lift value that gives the highest air velocity into the combustion chamber at different intake valve diameter. Two (2) different engine`s cylinder head with 23 mm diameter intake valve size and 27 mm diameter intake valve size are used in the simulation. Each valve size profile is tested with nine (9) different valve lift height profile from one (1) millimeter (mm) valve lift to nine (9) millimeter (mm) valve lift. For 23 mm intake valve size, at the openings of 1 mm to 5 mm intake valve height, non-uniform airflow is detected around the opening of the valve. The more uniform flow fluid is detected at the valve openings starting at 6 mm to 9 mm. Fluid pressure in combustion chamber increase significantly between 1mm to 5mm valve opening. But no significant change of the combustion chamber pressure is seen

when the valve lift is between 6mm and 9mm valve opening. For 27 mm intake valve size, at the openings of 1 mm to 3 mm intake valve height, non-uniform airflow is detected around the opening of the valve. The more uniform flow fluid is detected at the valve openings starting at 4mm to 9mm valve opening. Fluid pressure in combustion chamber increase significantly between 1mm to 3mm valve opening. But no significant change of the combustion chamber pressure is seen when the valve lift is between 4mm and 9mm. From the computational fluid dynamic simulations, result and analysis carried out, it was found that, for a 23 mm diameter valve size, the optimum valve lift required was 6 mm. Increasing the valve lift exceeds the 6mm value does not significantly increase the fluid volume entering into the engine cylinder during the intake cycle. For a 27 mm diameter valve size, the optimum valve lift required was 4 mm. Increasing the valve lift exceeds the 4mm value does not significantly increase the amount of fluid entering into the engine cylinder.

KAJIAN DINAMIK BENDALIR KEATAS KESAN BUKAAN INJAP TERHADAP HALAJU BENDALIR KE DALAM INJAP MASUKAN ENJIN PETROL

ABSTRAK

Tinggi bukaan injap masukan memainkan peranan yang amat penting dalam memastikan kuasa dan prestasi enjin pembakaran dalaman. Bukaan injap masukan yang terlalu rendah akan menyebabkan aliran udara ke dalam kebuk pembakaran menjadi tidak lancar dan mengurangkan jumlah udara yang memasuki kebuk pembakaran, seterusnya menyebabkan pembakaran dengan tenaga yang rendah. Walau bagaimanapun, meningkatkan nilai bukaan injap masukan melebihi nilai maksimum tidak akan memberikan apa-apa aliran bendalir tambahan ke dalam ruang pembakaran. Penggunaan bukaan injap yang lebih tinggi sering memerlukan tempoh camshaft yang lebih panjang dan meningkatkan beban enjin, yang boleh menjejaskan prestasi dan ketahanan enjin. Oleh itu, menentukan nilai angkat injap optimum adalah penting untuk mengekalkan keberkesanan dan prestasi enjin petrol. Kajian aliran bendalir di sekitar injap masukan dalam enjin pembakaran dalaman sukar dilakukan secara eksperimen disebabkan oleh kedudukan serta saiz komponen - komponen yang kecil yang bergerak pada kelajuan tinggi di dalam enjin. Oleh itu, penggunaan CFD merupakan kaedah terbaik bagi projek yang dijalankan ini. Analisis ini dijalankan untuk menentukan nilai bukaan injap optimum yang memberikan halaju udara tertinggi ke dalam ruang pembakaran pada diameter injap masukan yang berbeza. Dua (2) kepala silinder enjin dengan saiz injap pengambilan diameter 23 mm dan saiz injap pengambilan diameter 27 mm digunakan dalam simulasi. Setiap profil saiz injap diuji dengan sembilan (9) profil ketinggian bukaan injap yang berbeza dari satu (1) milimeter (mm) hingga sembilan (9) milimeter (mm). Untuk saiz injap masukan bersaiz 23 mm, pada bukaan injap masukan antara 1 mm hingga 5 mm, aliran udara yang tidak seragam dikesan sekitar injap. Aliran yang lebih seragam dikesan

pada bukaan injap bermula pada 6 mm hingga 9 mm. Tekanan kebuk pembakaran meningkat dengan ketara pada pembukaan injap antara 1mm hingga 5mm. Tetapi tiada perubahan ketara dalam tekanan ruang pembakaran boleh dilihat apabila bukaan injap antara 6mm hingga 9mm. Untuk saiz injap masukan bersaiz 27 mm, pada bukaan ketinggian injap masukan anara 1 mm hingga 3 mm, aliran udara yang tidak seragam dikesan sekitar pembukaan injap. Aliran yang lebih seragam dikesan pada bukaan injap bermula pada pembukaan injap antara 4mm hingga 9mm. Tekanan kebuk pembakaran meningkat dengan ketara antara pembukaan injap 1mm hingga 3mm. Tetapi tiada perubahan ketara dalam tekanan ruang pembakaran boleh dilihat apabila bukaan injap antara 4mm dan 9mm. Dari simulasi dinamik yang dijalankan, didapati bahawa, untuk injap masukan bersaiz 23 mm diameter, bukaan injap optimum yang diperlukan ialah sebanyak 6 mm. Peningkatan bukaan injap melebihi nilai 6mm tidak akan meningkatkan jumlah cecair masuk ke dalam ruang pembakaran dengan ketara. Untuk ukuran injap bersaiz 27 mm diameter, bukaan injap optimum yang diperlukan adalah 4 mm. Peningkatan bukaan injap melebihi nilai 4mm tidak akan meningkatkan jumlah bendalir masuk ke dalam ruang pembakaran dengan ketara.

ACKNOWLEDGEMENTS

I would like to extend my sincere appreciation and thanks to my project supervisor, Associate Prof. Ir. Dr. Nik Nazri Bin Nik Ghazali, Department of Mechanical Engineering, Faculty of Engineering, for his valuable time, effort, cooperation and guidance during the completion of this research project successfully.

Secondly, I am deeply indebted to the authorities of Faculty of Engineering, University of Malaya for providing me the necessary facilities to successfully carry put this research project work.

Finally, I would like to express my heartfelt thanks to my family, my parents, siblings and friends who were very understanding and supportive, and for their encouragement during the completion of this research project.

TABLE OF CONTENTS

LIST OF FIGURES

LIST OF TABLES

LIST OF SYMBOLS AND ABBREVIATIONS

ATDC	:	After Top Dead Centre
BTDC	:	Before Top Dead Centre
BTC	:	Bottom Dead Centre
CAD	:	Computer Aided Design
CFD	:	Computational Fluid Dynamic
EIVC	:	Early intake valve closing
ICE	:	Internal Combustion Engine
LIVC	:	Late intake valve closing
NOx	:	Nitrogen Oxides
PDF	:	Probability Density Function
RANS	:	Reynolds-average Navier-Stokes
RPM	:	Rotation per Minute
SAE	:	Society of Automotive Engineers
SOx	:	Sulfur Oxides
TDC	:	Top Dead Centre

LIST OF APPENDICES

CHAPTER 1: INTRODUCTION

Valve Lift is the amount of the valve is lifted off from its seat. High valve lift enables more air-fuel ratio to enter the combustion chamber, improving the performance of gasoline engine. Maximum intake valve lift plays great importance on performance of gasoline engines. Maximum valve lift is the highest intake valve opening that provide highest fluid flow to combustion chamber.

However, increasing the valve lift beyond the maximum valve lift value will not give any additional flow of fluid into the combustion chamber. Higher lift often requires longer camshaft duration and increase valve train work, which can affect the performance and durability of the engine. Determining the optimum valve lift value is crucial to maintain the effectiveness and performance of the gasoline engine.

1.1 Objective of the research project

This project was conducted to investigate the characteristics of the fluid movement within the intake valve during the intake duration of the internal combustion engine. Computational fluid dynamics analysis and simulation will be used to study the characteristics of air flow around intake valve at different camshaft lift and engine rotational speed.

The objectives of the project are:

i. To determine the highest valve lift value that gives the highest air velocity into the combustion chamber.
ii. To investigate the characteristics of the fluid movement within the intake valve during the intake duration.
iii. To investigate fluid movement around the intake valve opening during high engine rpm.

1.2 Scope of the research project

Computational fluid dynamics will be used in analysis and simulation of the project. The analysis will be conducted using single cylinder, single camshaft gasoline engine. Engine with 110cc capacity will be used as modelling. The analysis only to study the air flow through intake valve during engine intake stoke at different valve lift values. Two different valve face diameters will be used in the simulation which is 23mm and 27mm.

CHAPTER 2: LITERATURE REVIEW

2.1 Internal Combustion Engine

ICE is an engine that uses fossil fuel to convert chemical energy into mechanical energy. This energy conversion process requires a mixture of fire, air and heat. The air-fuel mixture at a specific ratio will be compressed by a mechanical system, so heat will be supplied through the spark plug. Expansion of mixture at high temperature and high pressure will transfer pressure, causing the mechanical movement into the engine by rotating shaft.

Most internal combustion engines are reciprocating engines. (W. Pulkrabek, 2004). This type of engine uses reciprocating pistons that move back and forth inside the engine cylinder. Reciprocating engines can consist of several pistons arranged in various configurations. The number and arrangement of the piston made based on the power and size of the engine required by the designer and the use of the engine. However, there are also engines that do not use a reciprocating piston system. For example, Wankel engine using rotating pistons and jet engines that use continuous combustion through engine blades.

Typically, spark-ignition internal combustion engines use fossil fuels to operate. This engine requires a specific air-fuel mixture to produce optimum energy. In addition, spark timing is also important to ensure that combustion can be carried out completely in the internal combustion engine. There are two (2) types of reciprocating engine; four-stroke and also two-stroke internal combustion engines.

2.2 Four (4) Cycle Gasoline Engine

Four-stroke engine uses four (4) cycles to complete the engine cycle; intake, compression, power and exhaust stroke. Each cycle has different roles and functions on the engine process.

Intake stroke refers to the process of admission of air and fuel into the engine cylinder. This stroke starts at piston T.D.C. and ends at piston B.D.C. At this point, the input valve will be opened while the exhaust valve will be closed. The piston will move downwards which will produce low pressure in the cylinder compared to the air pressure in the intake manifold. This pressure difference will result in the movement of the fluid into the cylinder.

Compression stroke refers to the air-fuel compression process inside the cylinder. The process starts as soon as the stroke intake ends at piston B.D.C and ends at piston T.D.C. At this point, both the intake valve and the exhaust valve are closed.

Power stroke refers to the ignition and combustion process of air-fuel in the cylinder. This process starts in the second round of the engine. At this point, combustion of fluid mixture will cause thermal expansion, thereby forcing the piston to move from T.D.C to B.D.C and rotating the crankshaft at the same time. At this point, both the intake valve and the exhaust valve are closed.

Exhaust stroke refers to the process of removing combustion results from engine cylinders. The exhaust valve is open and the piston moves from B.D.C to T.D.C, forcing combustion excess out from the engine.

The valves play a very important role in determining the speed of fluid flow in and out of the engine. ICE performance is much influenced by the timing, duration and lift of these valves.

2.2.1 Valve Timing

Four-stroke engines use valves to open and close at certain timing depending on engine cycle. The cams push the valves for a certain amount of time during each intake and exhaust cycle. Valve opening timing throughout the piston movement is very important in determining ICE performance. Research also shows valve closing timing have significant effect on emission level of an internal combustion engine (Jia, Xie, Wang, & Peng, 2011).

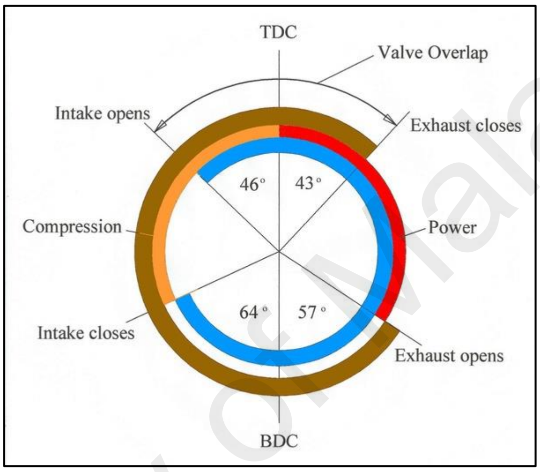

Figure 2.1: Valve Timing Chart (Dovat, 2018)

At high speed, large amounts of air-fuel are needed for combustion. Closing intake valve too soon will reduce the amount of air-fuel mixture entering combustion chamber, resulting decreasing performance (W. Pulkrabek, 2004). But, opening valves too long will affect engine performance at low speed.

To overcome this problem, the variable valve timing (VVT) system was introduced to improve engine performance during low and high rpm. Valves opening and closing timing will be adjusted according to engine speed without changing the valve duration. The VVT system was able to optimize the power and fuel consumption of the gasoline engine (Fontana & Galloni, 2009).

2.2.2 Valve Lift

Valve lift refers to maximum valve lifted off its seat at the cam lobe’s tip. It is measured with a dial gauge at the end of the valve stem (Figure 2.2). Meanwhile, Lobe Lift (Figure 2.3) is the amount that the highest point of cam lobe from the cam base circle. Opening the valves faster and higher will increase engine power. This condition can be achieved by changing the shape of the lobe cam to be higher and steep. However, such cam lobe will increase the cam duration, which will change the power curve shape of the engine.

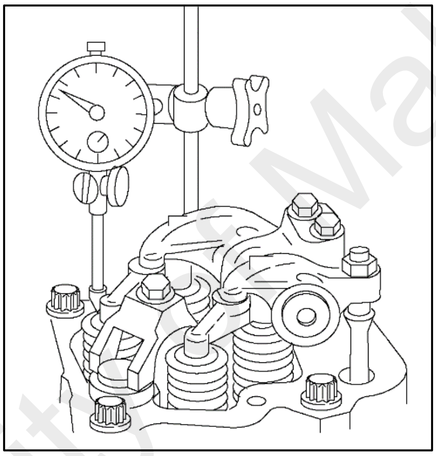

Figure 2.2: Valve Lift Measurement (Detroit, 2018)

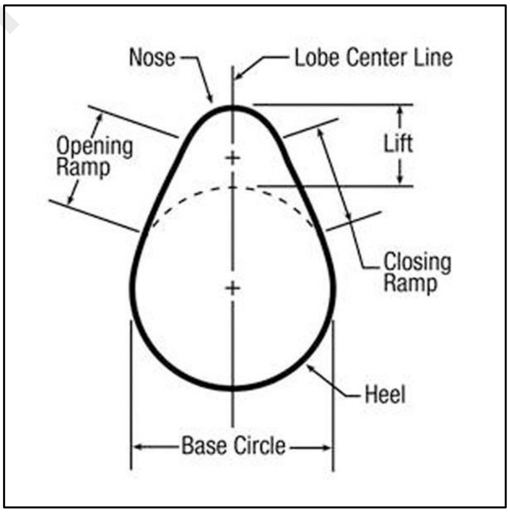

Figure 2.3: Cam Lobe Lift (Lubken, 2016)

2.2.3 Valve Duration

Valve duration is the amount of valve opening time, measured in crankshaft rotation angle. Valve duration is measured with a dial indicator and a degree wheel. Increasing duration keeps the valve open longer, and can increase engine power at high rpm. However, increasing valve duration will increase valve overlap.

2.2.4 Lobe Separation

Lobe separation is the angle of overlap between intake cam and exhaust cam (Figure 2.4). Lobe separation affects valve overlap, effecting the shape of engine's power curve.

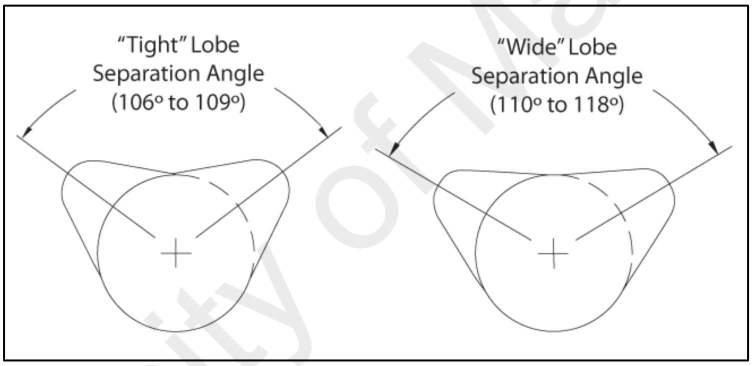

Figure 2.4 Lobe Separation Angle (Lunati, 2008)

2.2.5 Valve Overlap

Valve overlap is the condition of both intake and exhaust valves are open. Valve overlap happens just after the exhaust cycle and before the intake stroke takes place, and piston at T.D.C (Figure 2.5). Valve overlap is closely related to the lobe separation angle and cam duration. At high engine rotation speed, overlap enables the rush of exhaust gasses out the exhaust valve to help pull the fresh air/fuel mixture into the cylinder through the intake valve. Increasing overlap increases engines top-end power. However it will decrease engine's low-speed power and idle quality (W. Pulkrabek, 2004).

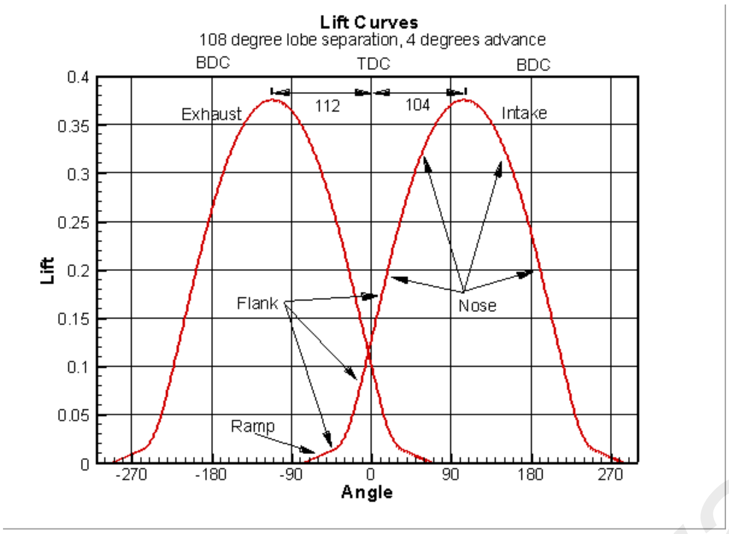

Figure 2.5: Valve Opening Curve (Young, 2007)

2.3 Cylinder pressure

Cylinder pressure is the pressure in the four-stroke engine cylinder during operation. The pressure during intake, compression, combustion and exhaust is important for the evaluation of engine performance.

2.3.1 Cylinder Pressure of Intake Stroke

During intake stroke, the piston movement creates an increase in volume in the engine cylinder. The sudden increase in the volume of engine cylinder will dramatically decrease air pressure inside the cylinder relative to atmospheric pressure. This pressure difference causes airflow into the cylinder.

At this point, the amount of fluid entering the engine cylinder depends on the intake path including intake manifold, throttle body and valve openings. Low-resistance intake pathways will increase fluid flow into the cylinder, thereby increasing the amount of air-fuel mixture to improve engine performance during combustion. Research shows that intake pathways giving a significant influence to tumble motion and turbulent intensity distribution in internal combustion engines (Falfari, Brusiani, & Pelloni, 2014). In addition, low fluid resistance will reduce work required during intake stroke.

2.3.2 Cylinder Pressure of Compression Stroke

During compression stroke, both the input and exhaust valves are closed when the piston moves from B.D.C to T.D.C, increasing the pressure in the decreased engine volume. Increased pressure inside the cylinder helps fuel evaporation in the air mixture. Until this process, the engine has not yet produced energy from fuel and only uses energy to operate

2.3.3 Cylinder Pressure of Combustion / Expansion Stroke

During the Combustion Stroke, burning air-fuel mixture instantly increase cylinder pressure in the combustion chamber. The pressure expansion will force the piston from T.D.C to B.D.C and create work to the engine. As the piston moving from T.D.C to B.D.C, the cylinder volume increases and cause the pressure to decrease.

2.3.4 Cylinder Pressure of Exhaust Stroke

During Exhaust Stroke, piston moving from B.D.C to T.D.C and exhaust valve is open. As the piston moving from B.D.C to T.D.C, the excess fluid in cylinder is forced out from cylinder through exhaust port. Less-restriction exhaust port will facilitate combustion excess from engine cylinder, reducing power usage during exhaust stroke.

2.4 Computational Fluid Dynamic of Internal Combustion Engine

ICE is a complex process involving thermochemistry reactions and the movement of fluid in internal geometry that is involved in engine components. This process occurs at a very fast and instantaneous rate. Fluid pathways, jet fuel formation, fluid mixing and fuel combustion are critical processes that are taken into account in the design stage to ensure that the engine is designed to have high efficiency and meet the standard emission standards.

There are several methods used in designing and analyzing engine performance. the use of CAD software is a common method at design stage. for analyzing engine performance, experimental methods using engine test bench and engine dynamometer can be used to obtain engine performance data. In addition, Computational fluid dynamics is a popular method for solving the fluid problem involved in the engine. the use of CFD allows engineers to identify the fluid characteristic throughout the process inside the engine.

However, the CFD method is a complex process, time consuming, and vulnerable to computation errors (Roberpj, 2018). The CFD method involving the use of very small mesh in large quantities in geometry causes a high computation load to the computer system. Normally, simplified 3D modeling is needed to ensure the simulation process can run perfectly.

Several simplified methods can be used to reduce the computational loads of the computer and also reduce the calculation time of CFD approach; depending on the objectives and the data needed from the CFD results.

2.4.1 Port Flow Analysis

In the port flow analysis, engine components are frozen in the desired position during the engine cycle. Simulation and analysis of fluid movement in engine cavity is done on 3d model produced in this condition. Since the analysis is only done on a particular position of the engine, port flow analysis reduces the computational load to the computer and reduces the time required to obtain the simulation results. To study the turbulence effect in the engine, the RANS analysis is sufficient to be used during the simulation.

2.4.2 Cold Flow Analysis

In cold flow simulation, an analysis is performed to study the movement of the fluid during engine operations. At this point, fluid movement, fuel injection and air-fuel mixing process can be analyzed without involving any chemical and combustion processes. The purpose of this simulation is to investigate the movement of the fluid inside the engine during engine's operation. Through this analysis, flow characteristics around intake and exhaust valve during opening and closing can be observed. In addition, the turbulence effect in the engine volume can also be seen during the movement of the piston.

Providing CFD models for cold flow analysis results in additional work in determining the information required for analysis. In this simulation, the movement of each component of the engine needs to be specified. The valve and piston movement must be set up as a real engine operation. The use of UDF parameters requires analysts to prepare a complete model before the analysis can be done. Since component movement is involved during the simulation, dynamic mesh must be used in simulation. The use of dynamic mesh causes simulation to be time consuming. This is because the computer is forced to break every mesh movement into a separate calculation, causing the computation load to increase.

2.4.3 Combustion Simulation

The combustion simulation involves analysis of the combustion process in the engine. at this point, only the piston movements occur in the cylinder while the valves are closed. Dynamic meshing in combustion simulation only involves piston movement. This analysis is less complicated compared to port flow and cold flow analysis.

To carry out combustion simulations, detailed chemical reactions must be used during analysis. The use of the correct chemical reaction model during the simulation is important to produce good simulation results. However, the use of this complex analysis will increase the calculation time and computation load.

2.4.4 Full Cycle Simulations

Full cycle simulation involves engine analysis at all stages of the engine cycle. This simulation involves the movement of engine components, flow movements in and out of the engine cavity and all the chemical reaction processes and combustion involved. The use of full cycle analysis allows the overall performance evaluation of the engine during operation can be performed. Valve movement, piston, fluid movement, fuel injection pattern, fuel mix pattern, flame propagation, power estimation, pollutant and exhaust gas movement can be analyzed comprehensively. However, geometry preparation for full cycle are very complex. High level of expertise is required to make sure the simulation can be carried out successfully.

Preparation of model geometry will include all engine components from intake manifold, ports, valves, combustion chamber, pistons, cylinder and exhaust port. Meshing all the components will be challenging and difficult to perform especially with dynamic meshing involved in the simulation. Preparing the solver set up will require huge amount of efforts to specify UDF parameter of each moving components, combustion propagation settings, chemical reaction equation, turbulence approach and pollutant parameter setting.

CHAPTER 3: METHODOLOGY

3.1 Introduction

Port flow analysis will be used in simulation. Through this method fluid studies will be conducted during the maximum intake stroke of the gasoline engine. At this point, the piston is located at B.D.C while the intake valve is at maximum lift. Cold flow analysis method will also be used in the simulation. Through this method, air properties will be used as a fluid without the involvement of air - fuel mixture properties.

Figure 3.1 shows the project methodology used during this project study. This work step is used as a guide to ensure a systematic and organized study is implemented.

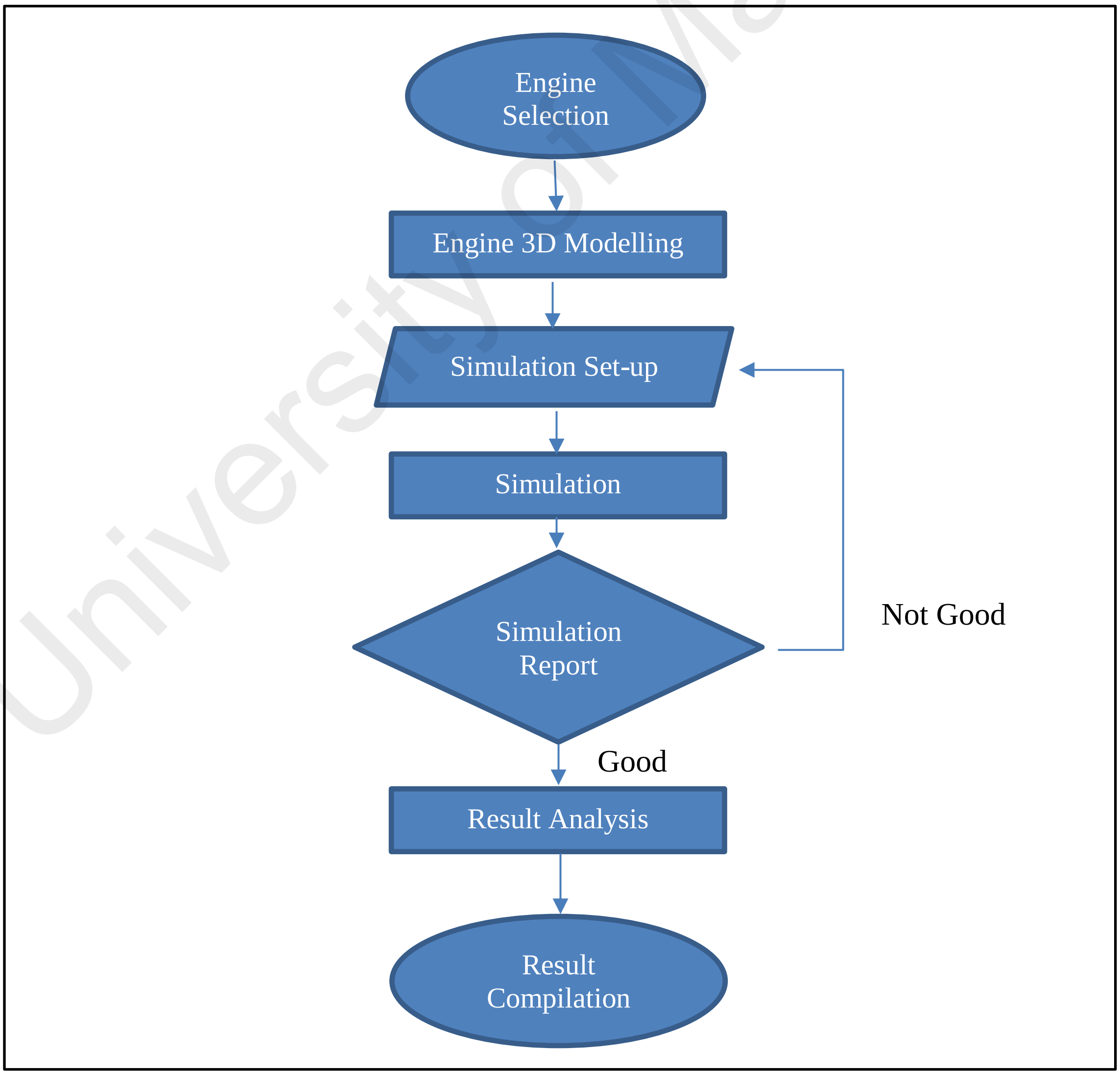

Figure 3.1: Project Methodology

3.2 Simulation Model

Engine models are taken from real engine specifications and developed in Solidworks software to produce 3D models for the simulation. A 100-centimeter cubic (cc) capacity of four (4) stroke, single cylinder, single overhead cam engine with 50mm bore and 49mm stoke is used as the engine model. Only the air cavity from intake manifold, inlet valve and cylinder are developed. To reduce computational burden, simulation will be carried out with only half of the model (Figure 3.2). The simulation will be done with the section face as symmetry plane during simulation.

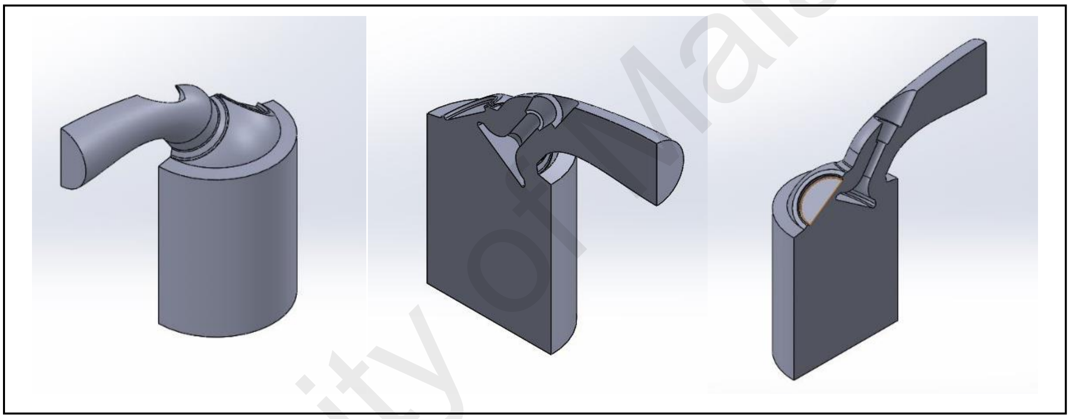

Figure 3.2: Air Cavity of Model Engine

Two (2) different engine`s cylinder head with 23 mm intake diameter valve size (Figure 3.3) and 27 mm diameter valve size (Figure 3.4) will be tested in the simulation. Each valve size profile will be tested with nine (9) different valve lift height profile from one (1) millimeter (mm) valve lift to nine (9) millimeter (mm) valve lift (Figure 3.5). Fluid flow velocity at the intake valve opening of each valve height configuration will be evaluated in each simulation. The fluid velocity changes in each valve configuration will be analyzed. The velocity profile of the fluid flow will be analyzed.

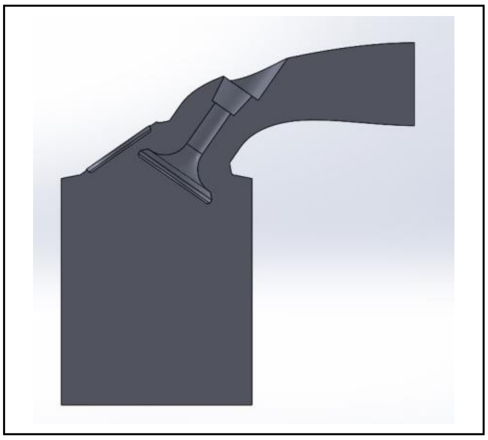

Figure 3.3: Engine Model of 23mm Intake Valve Diameter

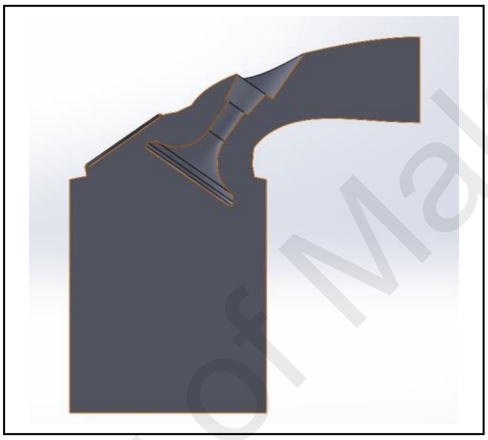

Figure 3.4: Engine Model of 27mm Intake Valve Diameter

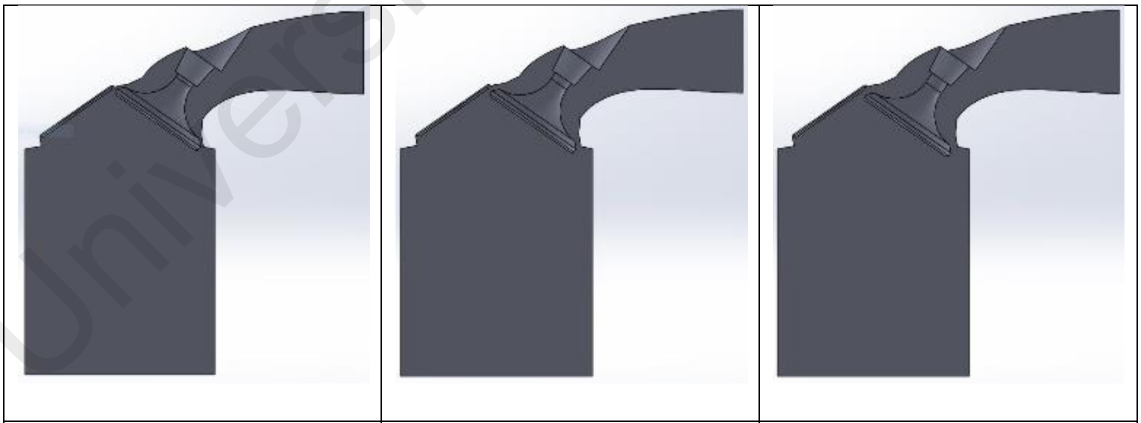

1mm Valve Lift	2mm Valve Lift	3mm Valve Lift

Figure 3.5: Valve Lift Height Configurations

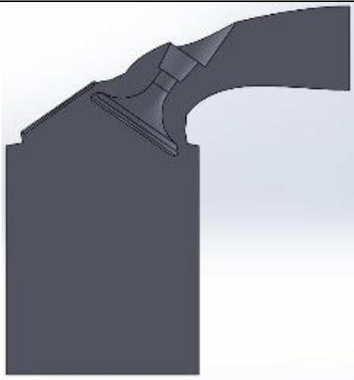	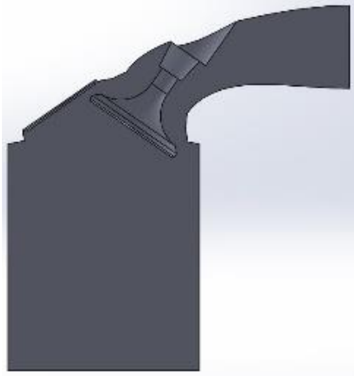	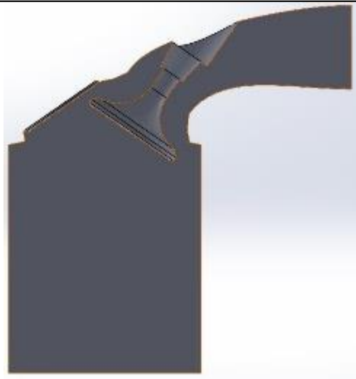
4mm Valve Lift	**5mm Valve Lift**	**6mm Valve Lift**
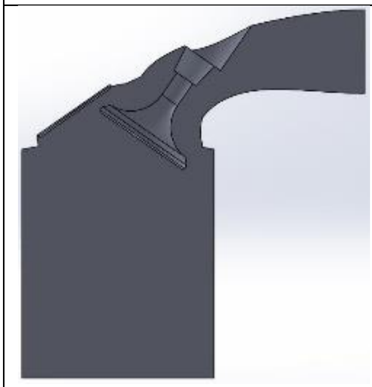		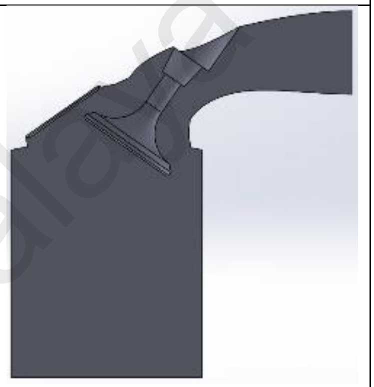
7mm Valve Lift	**8mm Valve Lift**	**9mm Valve Lift**

Figure 3.5: Valve Lift Height Configurations (continued)

3.3 Simulation Preparation

The developed model is imported into Ansys Fluent software. Before the simulation, some preparation must be done to ensure the simulation can be done smoothly. Boundary conditions is applied on the model surface as Figure 3.6.

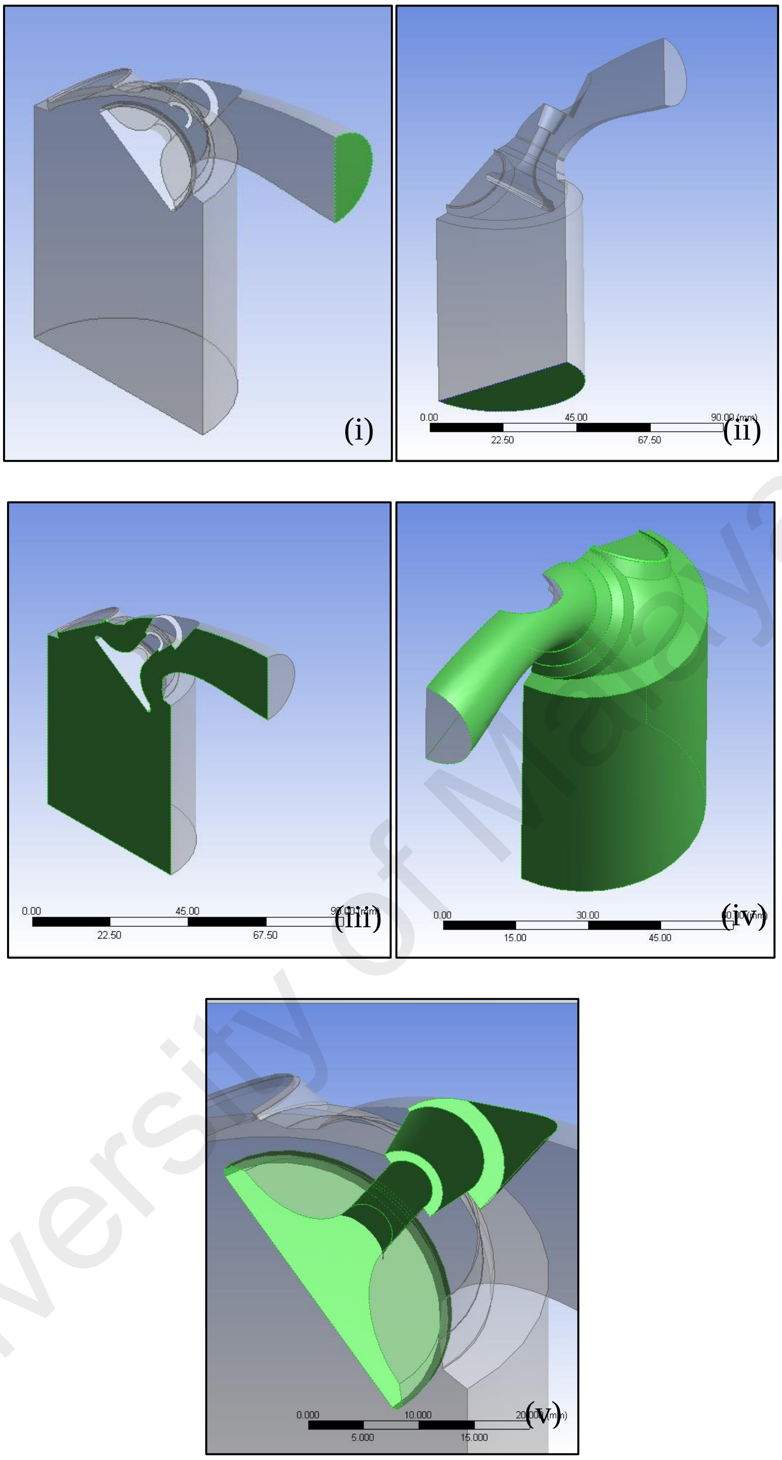

Figure 3.6: Geometry Conditions

The intake manifold surface (i) is defined as pressure inlet. The piston surface (ii) is set as outlet velocity. The sectioned plane (iii) is defined as symmetrical wall. The surface of the outer cylinder (iv) and valve surface (v) is set as a wall.

The intake pressure entered through the intake manifold is set as atmospheric pressure of 1 atm. The simulation is done at the engine rotation at around 10,000 rpm. Since the simulations by port flow and cold flow analysis are performed, the piston and valves are considered to be in static position at B.D.C. At this position, the intake stroke is at maximum state. Through the piston and bore size of the model, the mass flow rate through cylinder cross section is estimated through the calculation as shown below.

$$Bore, d = 50\ mm \tag{3.1}$$

$$Cylinder\ cross\ section, A = \pi j^2 = \pi(25x10^{-3}m)^2 = 1.964x10^{-3}m^2 \tag{3.2}$$

$$Target\ engine\ speed, w = 10{,}000\ rpm = 1047\ \ rad/s \tag{3.3}$$

$$Air\ density, \rho = \ 1.225\ \ kg/m^3 \tag{3.4}$$

$$Stroke\ velocity, v = rw = 25.918\ \ m/s \tag{3.5}$$

$$Mass\ flow\ rate, m = \rho vA = 0.0623\ \ kg/s \tag{3.6}$$

Model meshing is carried out to the entire model. Selection of mesh size is done so that simulation result obtained is accepted. The use of large mesh size causes less precise simulation results. However, the too small mesh sizes may cause an increase in computational time by the software. The size of the mesh for each simulation model is set to be equal to ensure uniform simulation results. Figure 3.7 shows model mesh generated for the simulations.

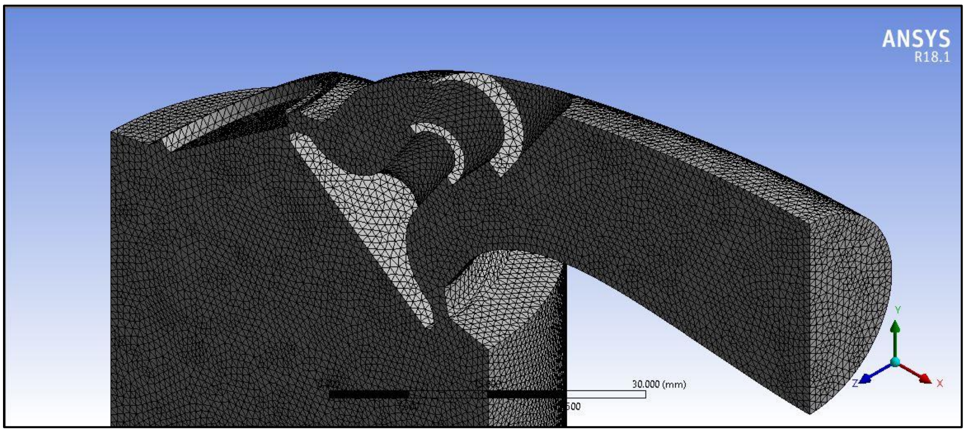

Figure 3.7: Model Mesh

Simulation calculation is carried out to achieve iteration by 3%. In most engineering applications, a 3% error is applicable for acceptance as a test result (Bong, 2011). Figure 3.8 below shows the stopping criteria for iteration cycle in the simulation.

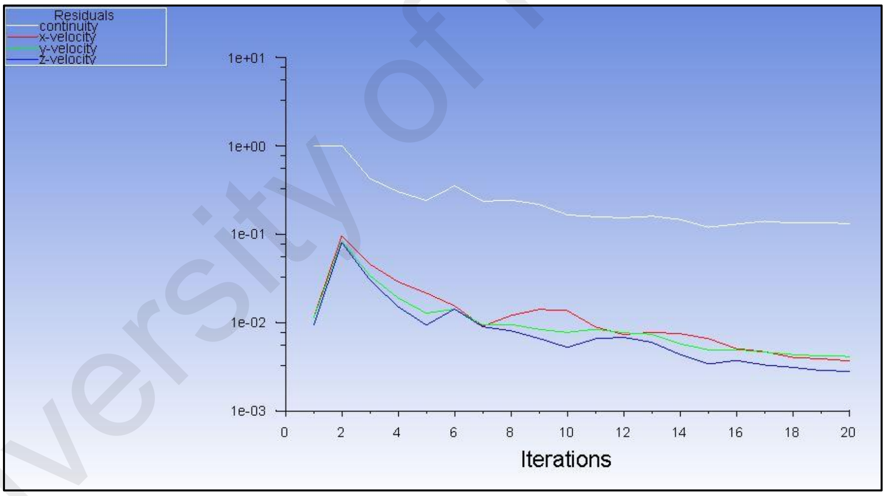

Figure 3.8: Stopping Criteria

3.4 Result Preparation

To analyze simulation results, the calculated data is graphically evaluated. The two main data to be analyzed are velocity magnitude (Figure 3.9) and pressure contour (Figure 3.10) inside the cylinder. velocity and pressure differences in all models will be analyzed and the results of the study will be investigated.

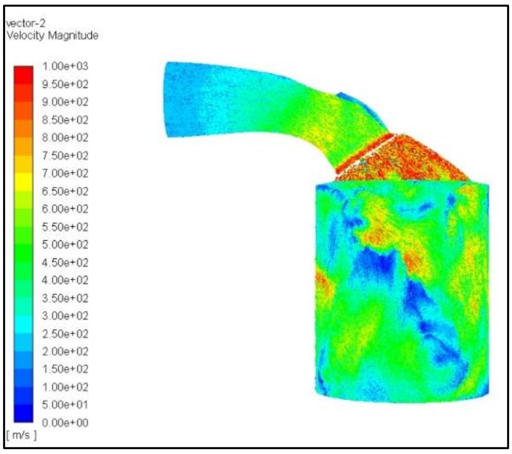

Figure 3.9 Velocity Magnitude

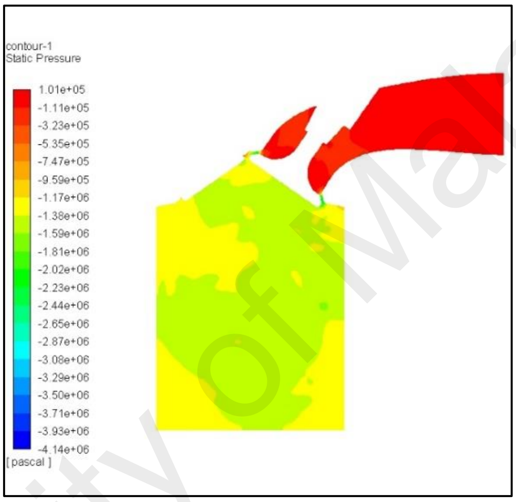

Figure 3.10 Pressure Contour

CHAPTER 4: RESULTS

4.1 Result for 23 mm Intake Valve Diameter

In this chapter, the results of the simulation of valve lifts opening from 1 mm to 9 mm for valve 23 mm diameter intake valve size will be presented.

4.1.1 1 mm Valve Lift Height

Figure 4.1 shows the velocity results of the simulation for the 1mm valve lift. The focus will be on the fluid velocity around the intake valve located in the combustion chamber section as the Figure 4.2.

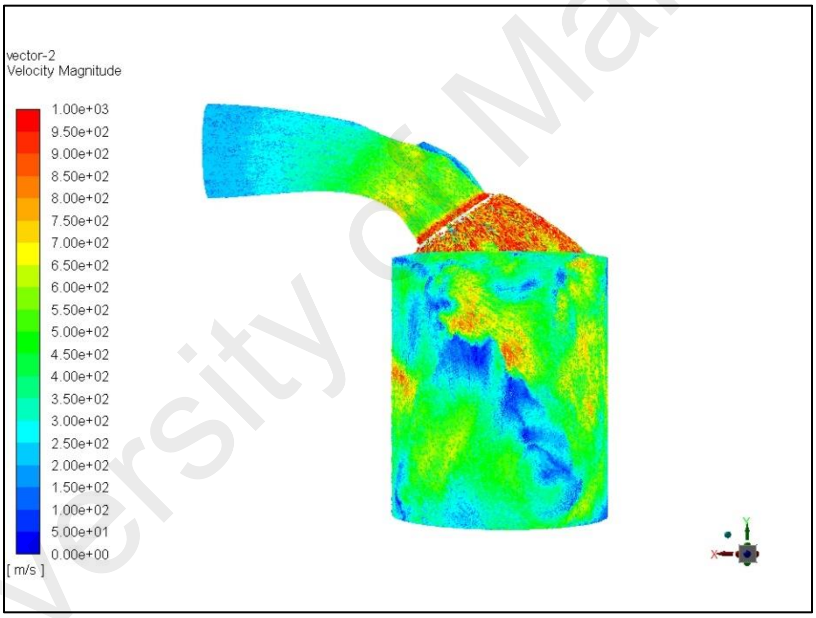

Figure 4.1: Velocity Profile of 1mm Intake Valve Lift

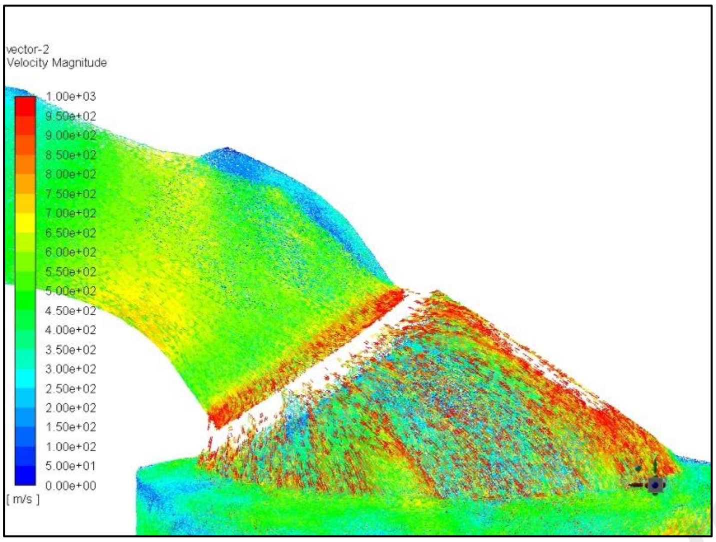

Figure 4.2: Fluid Velocity Around the 23 mm Intake Valve at 1 mm Lift

Figure 4.2 shows fluid velocity entering the combustion chamber through the intake valve. At 1mm valve opening, the fluid velocity around the valve opening is at a large range between 1.5 x 10^2 m/s to 1x 10^3 m/s.

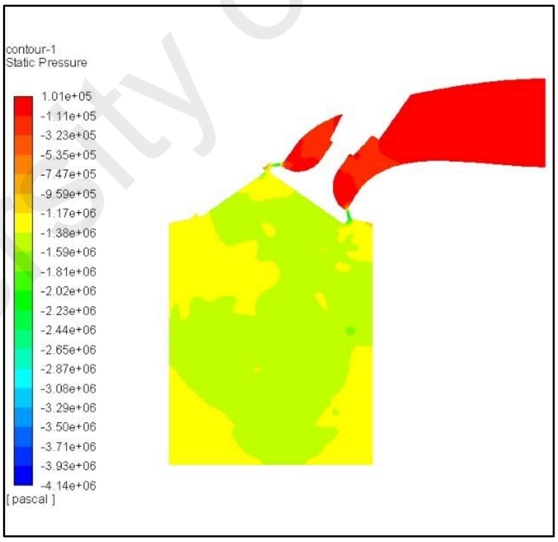

Figure 4.3: Pressure Contour of 23 mm Intake Valve Lift at 1 mm Lift

Figure 4.3 shows the pressure contour of the cylinder during the 1mm valve opening. At this point, it is found that the cylinder pressure is between -1.38 x 10^6 Pa to -1.17 x 10^6 Pa.

4.1.2 2 mm Valve Lift Height

The Figure 4.4 shows the velocity results of the simulation for the 2mm valve lift. The focus will be on the fluid velocity around the intake valve located in the combustion chamber section as the Figure 4.5.

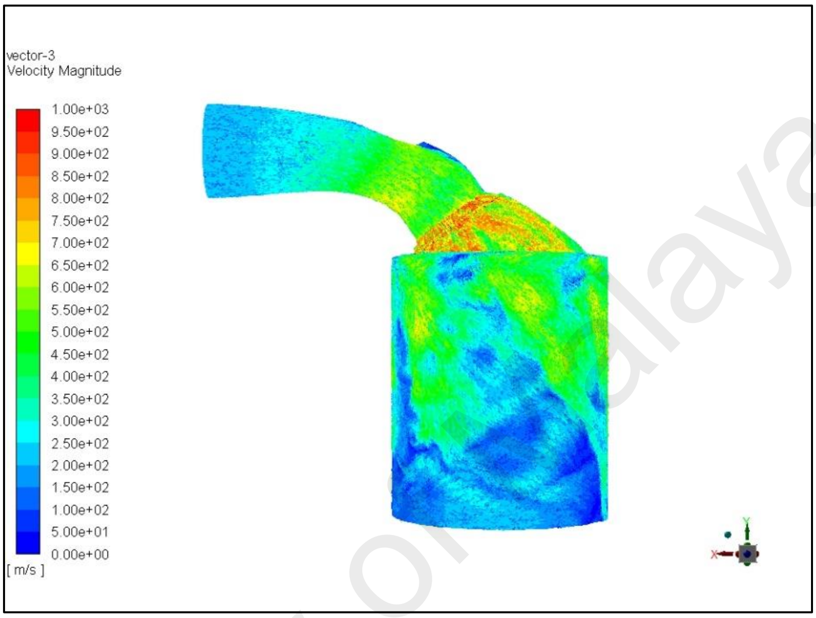

Figure 4.4 :Velocity Profile of 2mm Intake Valve Lift

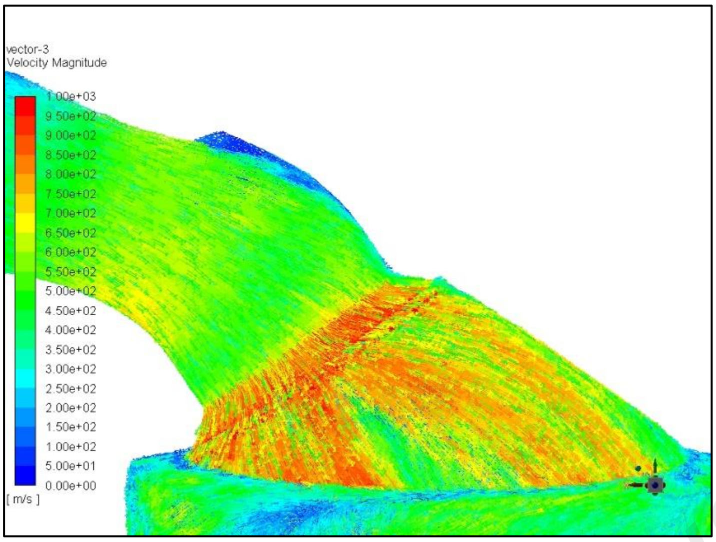

Figure 4.5: Fluid Velocity Around the 23 mm Intake Valve at 2 mm Lift

Figure 4.5 shows fluid velocity entering the combustion chamber through the intake valve. At 2mm valve opening, the fluid velocity around the valve opening is varies between 4.0 x 10^2 m/s to 1x 10^3 m/s.

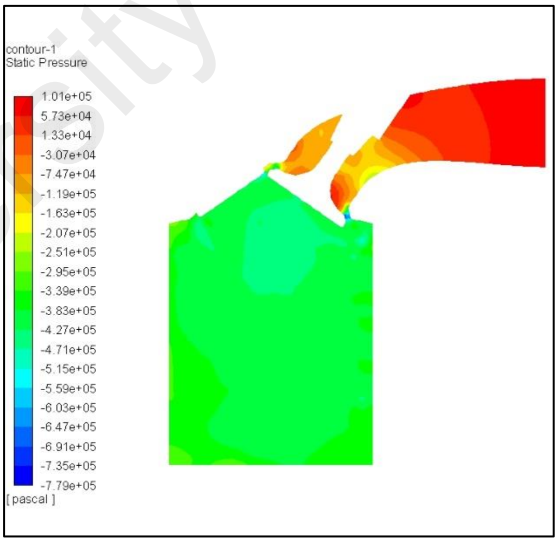

Figure 4.6: Pressure Contour of 23 mm Intake Valve Lift at 2 mm Lift

Figure 4.6 shows the pressure contour of the cylinder during the 2mm valve opening. At this point, it is found that the cylinder pressure is between -4.71 x 10^5 Pa to -4.27 x 10^5 Pa.

4.1.3 3 mm Valve Lift Height

Figure 4.7 shows the velocity results of the simulation for the 23 mm intake valve at 3 mm valve lift.

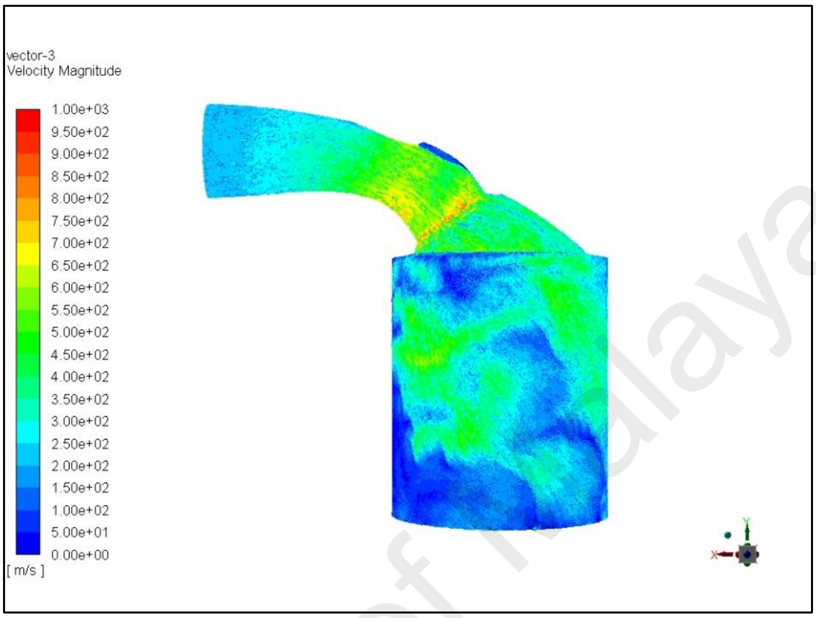

Figure 4.7: Velocity Profile of 23 mm Intake Valve at 3 mm Lift

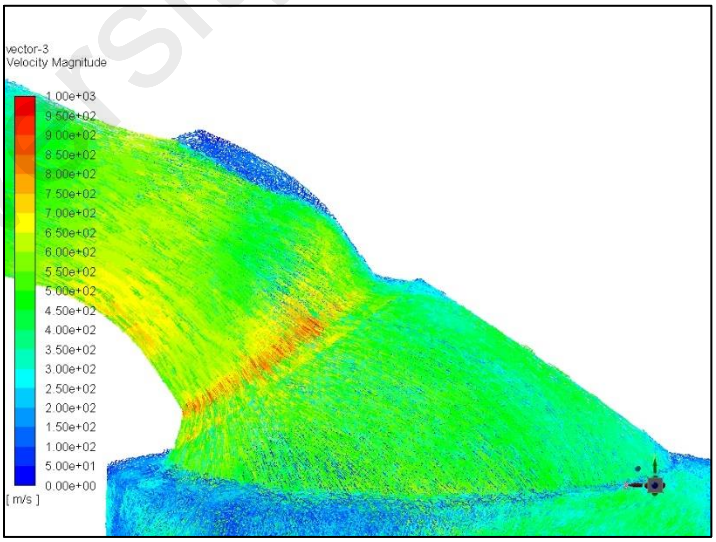

Figure 4.8: Fluid Velocity Around the 23 mm Intake Valve at 3 mm Lift

Figure 4.8 shows fluid velocity entering the combustion chamber through the intake valve. At 3 mm valve opening, the fluid velocity around the valve opening is varies

between 2.0 x 10^2 m/s to 6.0 x 10^2 m/s. However, there is a small area with high velocity profile that can be seen on the nearby valve seat.

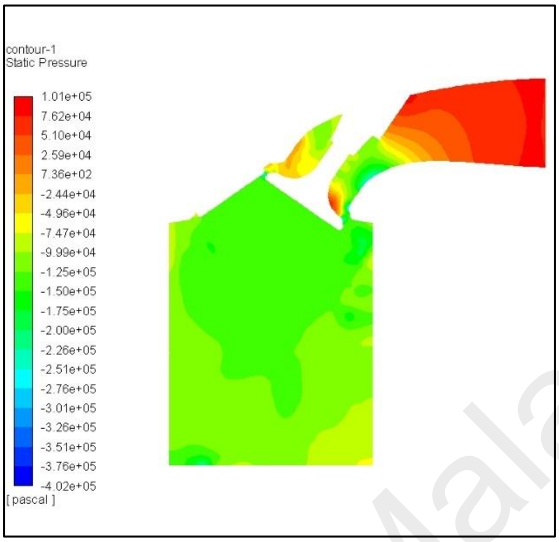

Figure 4.9: Pressure Contour of 23 mm Intake Valve Lift at 3 mm Lift

Figure 4.9 shows the pressure contour of the cylinder during the 3 mm valve opening. At this point, it is found that most of the cylinder pressure is between -1.75 x 10^5 Pa to -1.25 x 10^5 Pa.

4.1.4 4 mm Valve Lift Height

Figure 4.10 shows the velocity results of the simulation for the 23 mm intake valve at 4 mm valve lift.

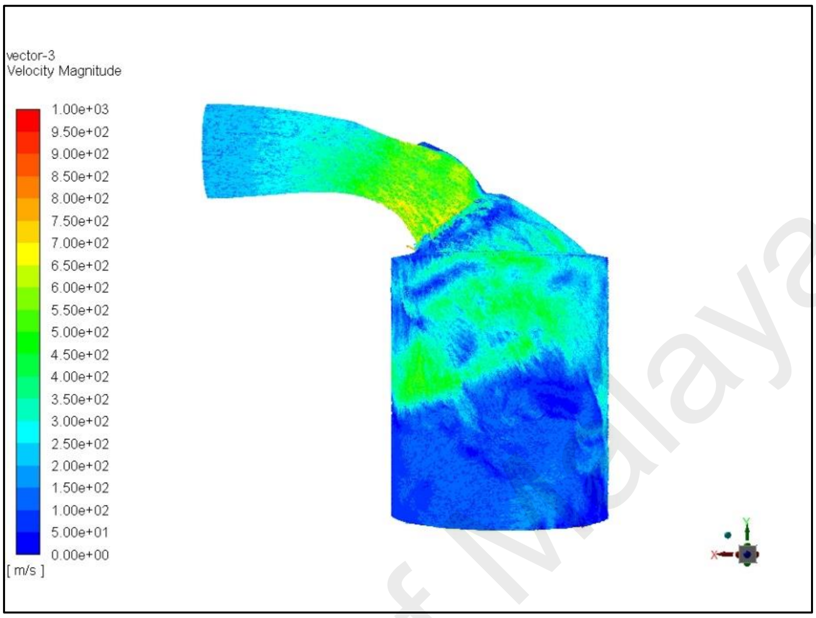

Figure 4.10: Velocity Profile of 23 mm Intake Valve at 4 mm Lift

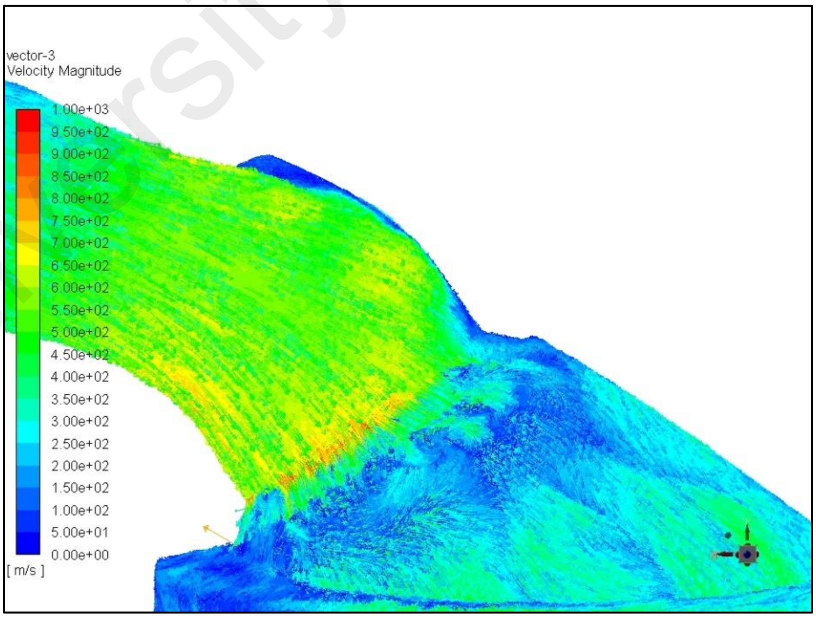

Figure 4.11: Fluid Velocity Around the 23 mm Intake Valve at 4 mm Lift

Figure 4.11 shows fluid velocity entering the combustion chamber through the intake valve. At 4 mm valve opening, the fluid velocity around the valve opening is varies

between 1.5 x 10^2 m/s to 3.5 x 10^2 m/s. However, there is a small area with high velocity profile that still can be seen on the nearby valve seat.

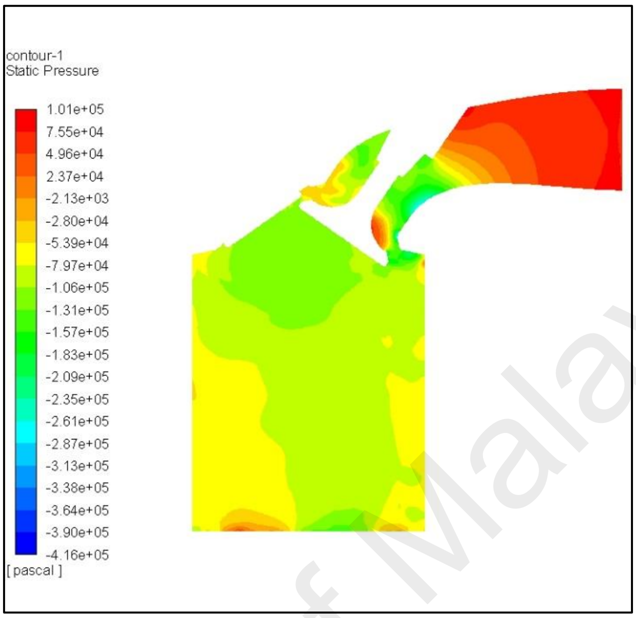

Figure 4.12: Pressure Contour of 23 mm Intake Valve Lift at 4 mm Lift

Figure 4.12 shows the pressure contour of the cylinder during the 4 mm valve opening. At this point, it is found that most of the cylinder pressure is between -1.06 x 10^5 Pa to -7.97 x 104 Pa.

4.1.5 5 mm Valve Lift Height

Figure 4.7 shows the velocity results of the simulation for the 23 mm intake valve at 5 mm valve lift.

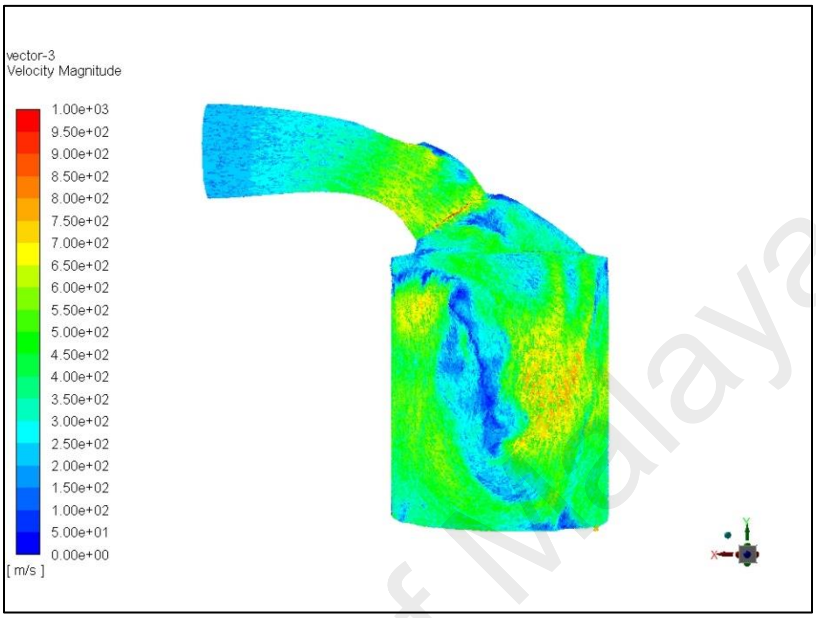

Figure 4.13: Velocity Profile of 23 mm Intake Valve at 5 mm Lift

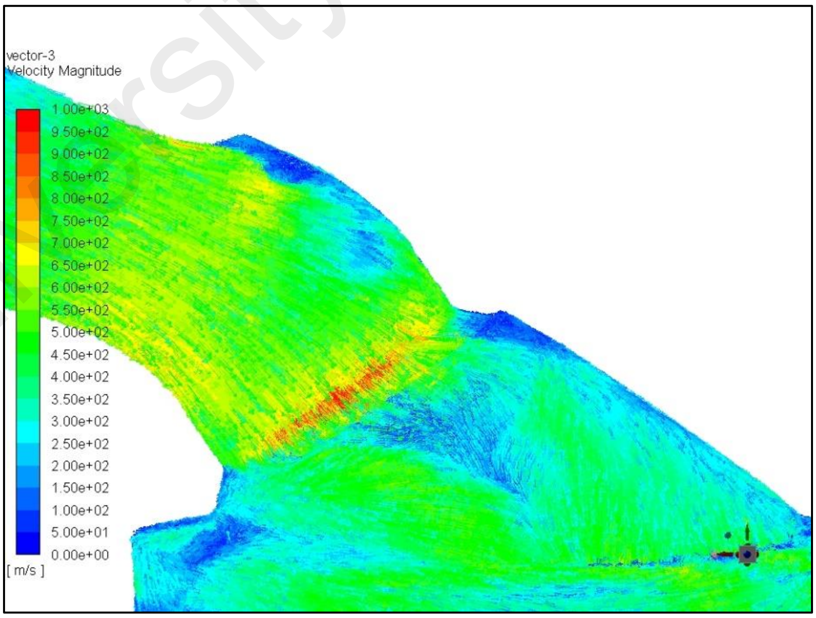

Figure 4.14: Fluid Velocity Around the 23 mm Intake Valve at 5 mm Lift

Figure 4.14 shows fluid velocity entering the combustion chamber through the intake valve. At 5 mm valve opening, the fluid velocity around the valve opening is varies

between 1.5 x 10^2 m/s to 5.5 x 10^2 m/s. However, there is a small area with high velocity profile that still can be seen on the nearby valve seat.

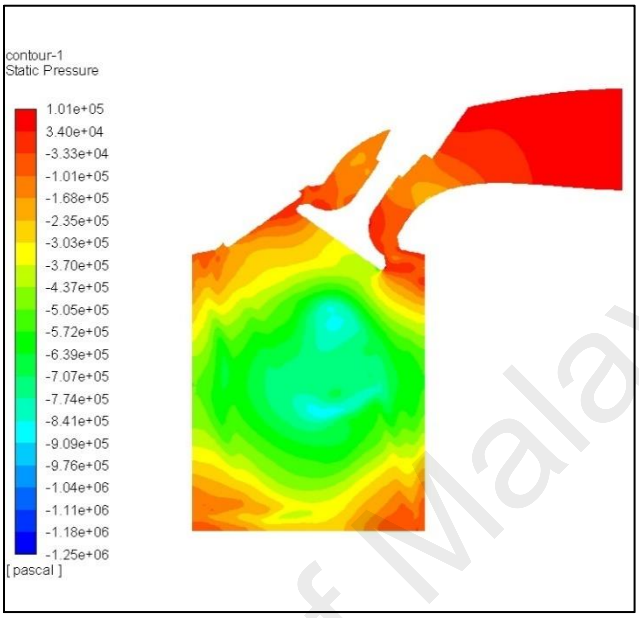

Figure 4.15: Pressure Contour of 23 mm Intake Valve Lift at 5 mm Lift

Figure 4.15 shows the pressure contour of the cylinder during the 5 mm valve opening. At this point, it is found that most of the cylinder pressure is between -5.72 x 10^5 Pa to -3.03 x 104 Pa.

4.1.6 6 mm Valve Lift Height

Figure 4.16 shows the velocity results of the simulation for the 23 mm intake valve at 6 mm valve lift.

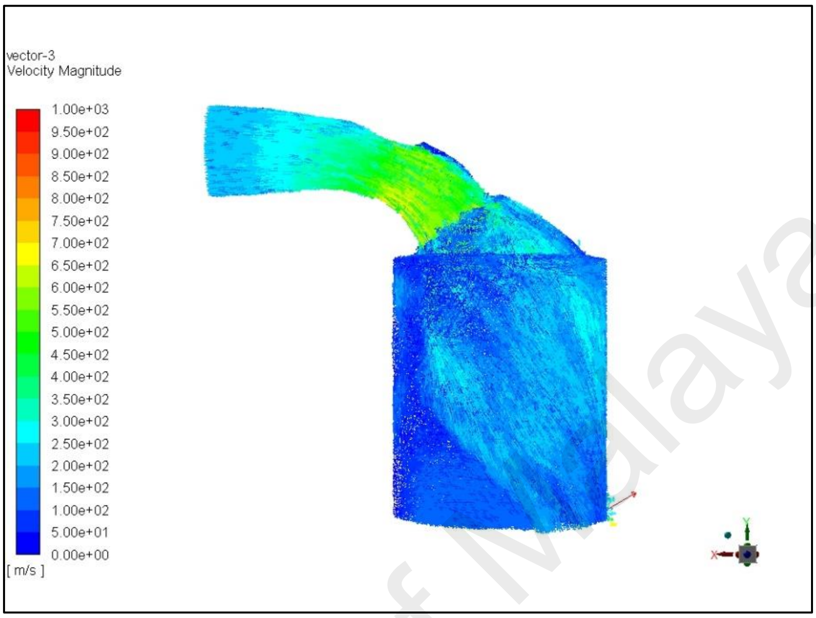

Figure 4.16: Velocity Profile of 23 mm Intake Valve at 6 mm Lift

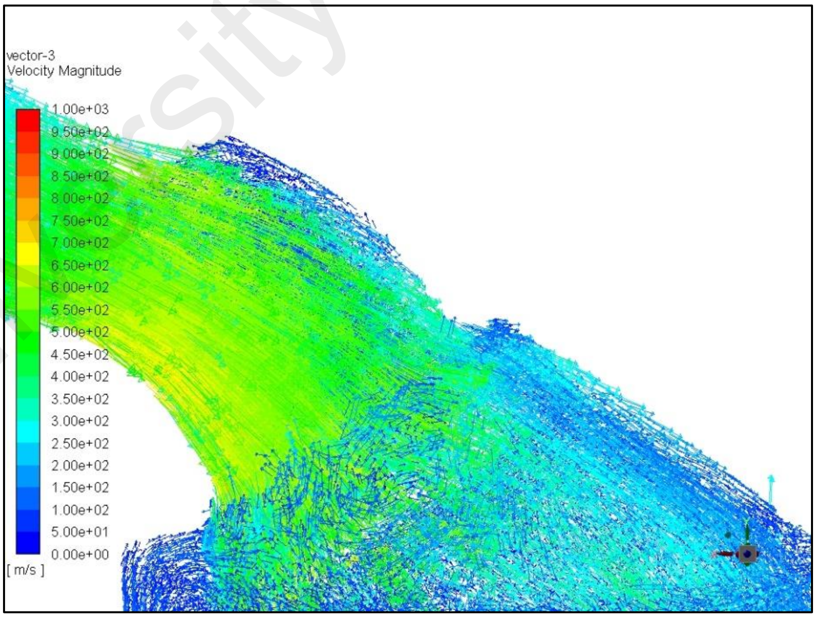

Figure 4.17: Fluid Velocity Around the 23 mm Intake Valve at 6 mm Lift

Figure 4.17 shows fluid velocity entering the combustion chamber through the intake valve. At 6 mm valve opening, the fluid velocity around the valve opening is varies

between 1.5 x 10^2 m/s to 3.0 x 10^2 m/s. However, at this lift value, the small area with high velocity profile nearby valve seat is completely vanished.

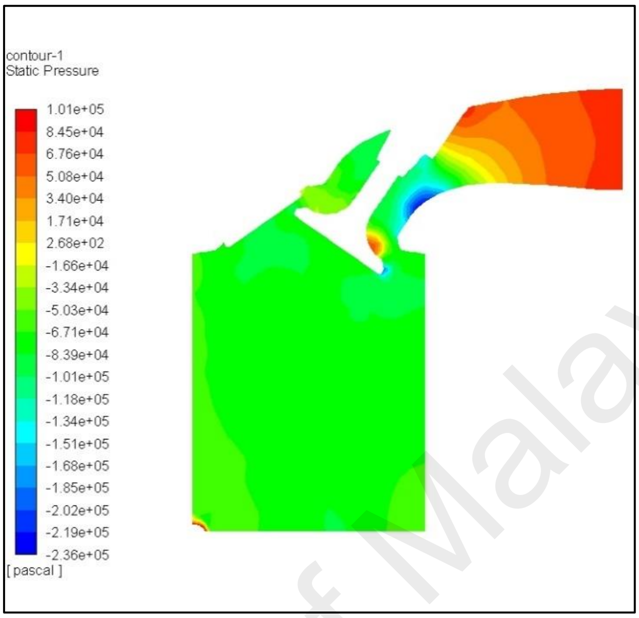

Figure 4.18: Pressure Contour of 23 mm Intake Valve Lift at 6 mm Lift

Figure 4.18 shows the pressure contour of the cylinder during the 6 mm valve opening. At this point, it is found that most of the cylinder pressure is between -8.39 x 10^4 Pa to -6.71 x 10^4 Pa.

4.1.7 7 mm Valve Lift Height

Figure 4.19 shows the velocity results of the simulation for the 23 mm intake valve at 7 mm valve lift.

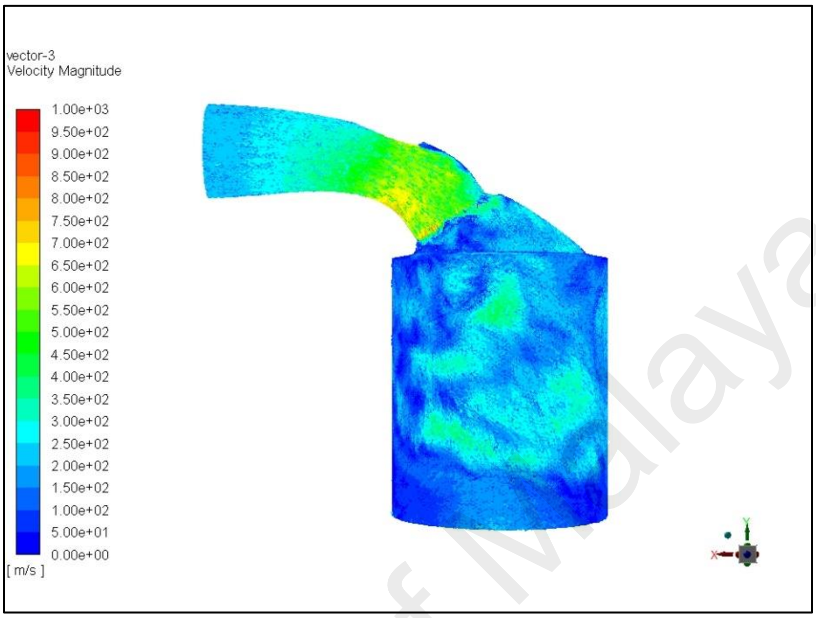

Figure 4.19: Velocity Profile of 23 mm Intake Valve at 7 mm Lift

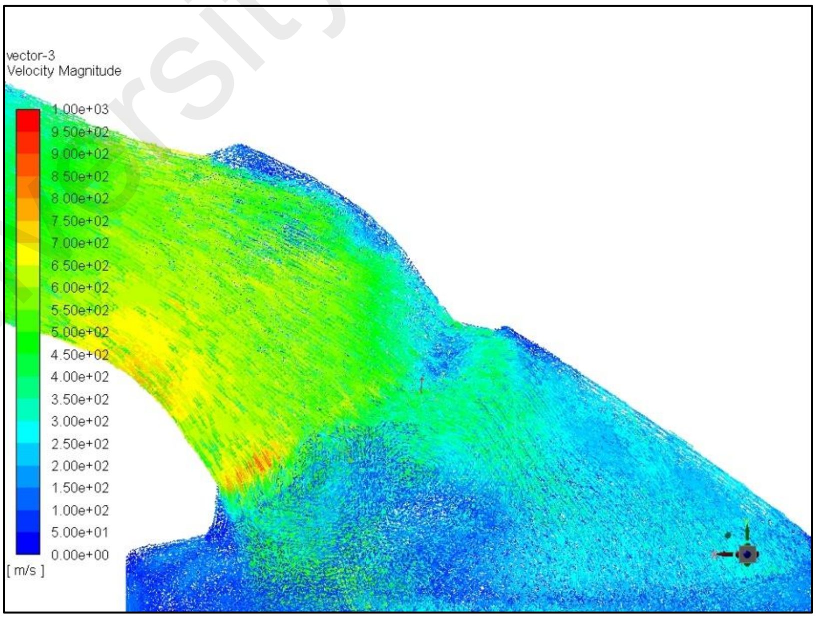

Figure 4.20: Fluid Velocity Around the 23 mm Intake Valve at 7 mm Lift

Figure 4.20 shows fluid velocity entering the combustion chamber through the intake valve. At 7 mm valve opening, the fluid velocity around the valve opening is varies

between 1.5 x 10^2 m/s to 3.0 x 10^2 m/s. However, at this lift value, the small area with high velocity profile nearby valve seat is completely vanished.

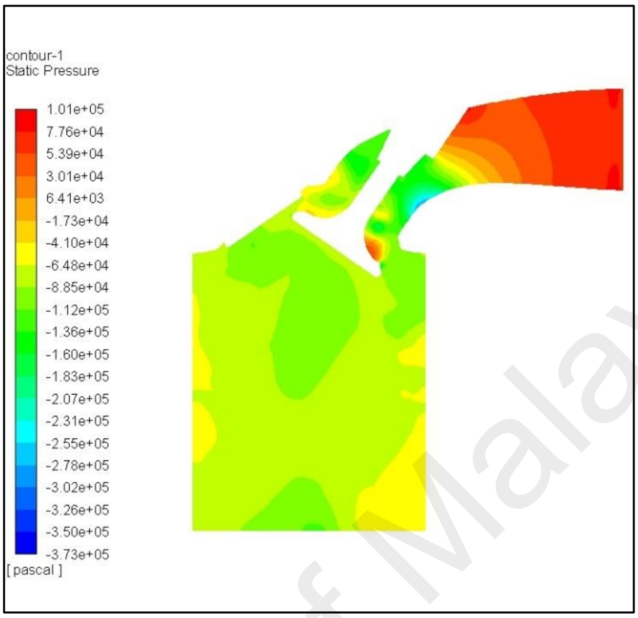

Figure 4.21: Pressure Contour of 23 mm Intake Valve Lift at 7 mm Lift

Figure 4.21 shows the pressure contour of the cylinder during the 7 mm valve opening. At this point, it is found that most of the cylinder pressure is between -8.85x 10^4 Pa to -6.48 x 10^4 Pa.

4.1.8 8 mm Valve Lift Height

Figure 4.22 shows the velocity results of the simulation for the 23 mm intake valve at 8 mm valve lift.

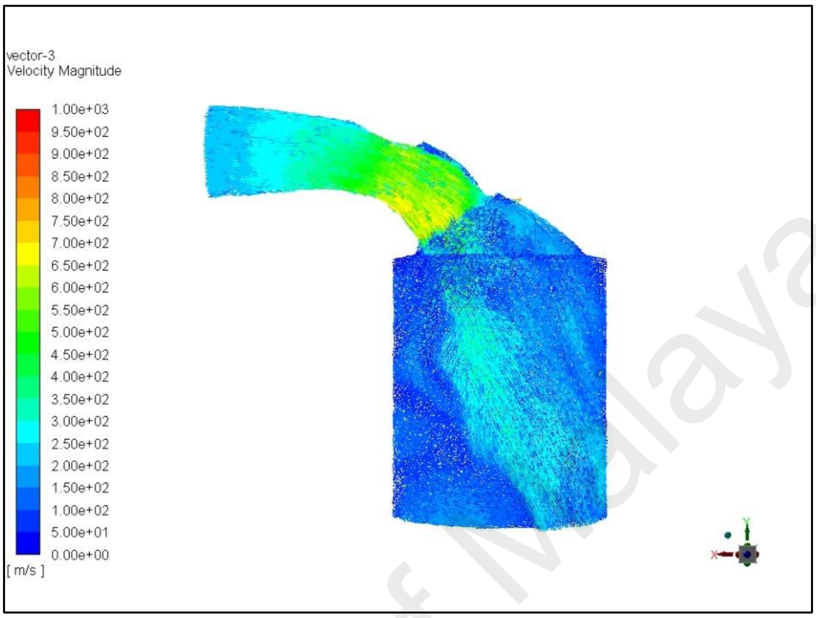

Figure 4.22: Velocity Profile of 23 mm Intake Valve at 8 mm Lift

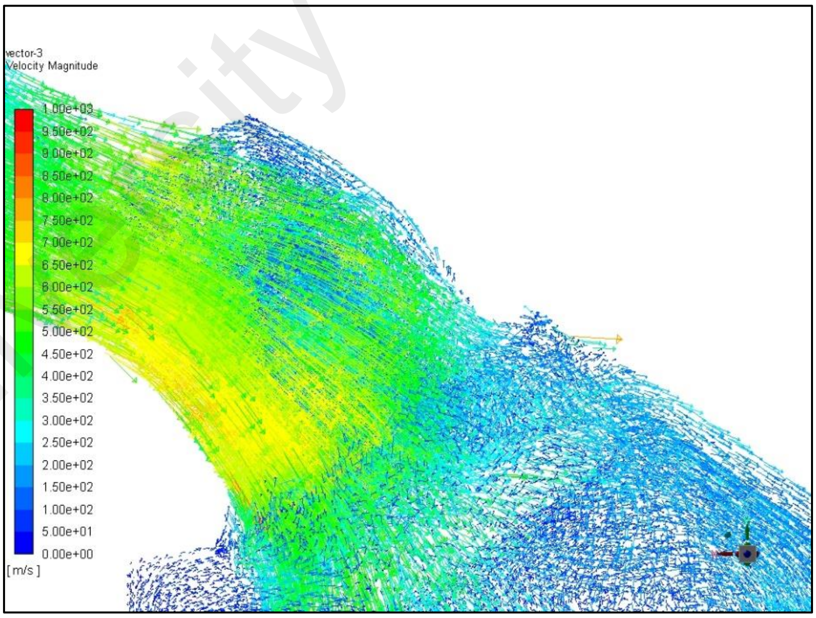

Figure 4.23: Fluid Velocity Around the 23 mm Intake Valve at 8 mm Lift

Figure 4.23 shows fluid velocity entering the combustion chamber through the intake valve. At 8 mm valve opening, the fluid velocity around the valve opening is varies

between 1.5 x 10^2 m/s to 3.0 x 10^2 m/s. However, at this lift value, the small area with high velocity profile nearby valve seat is completely vanished.

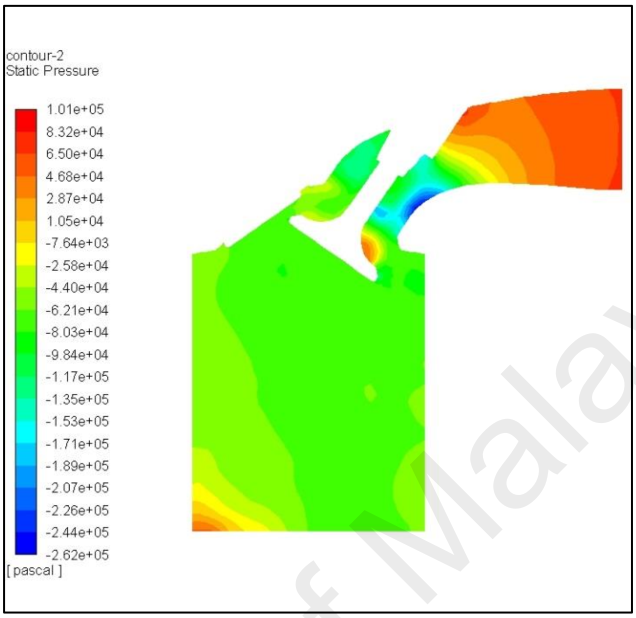

Figure 4.24: Pressure Contour of 23 mm Intake Valve Lift at 8 mm Lift

Figure 4.24 shows the pressure contour of the cylinder during the 8 mm valve opening. At this point, it is found that most of the cylinder pressure is between -8.03x 10^4 Pa to -4.40 x 10^4 Pa.

4.1.9 9 mm Valve Lift Height

Figure 4.25 shows the velocity results of the simulation for the 23 mm intake valve at 9 mm valve lift.

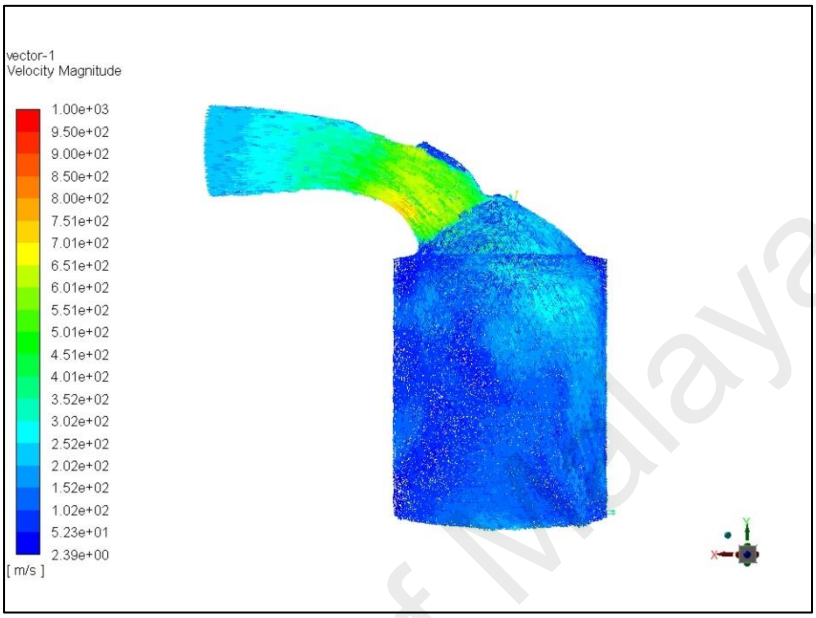

Figure 4.25: Velocity Profile of 23 mm Intake Valve at 9 mm Lift

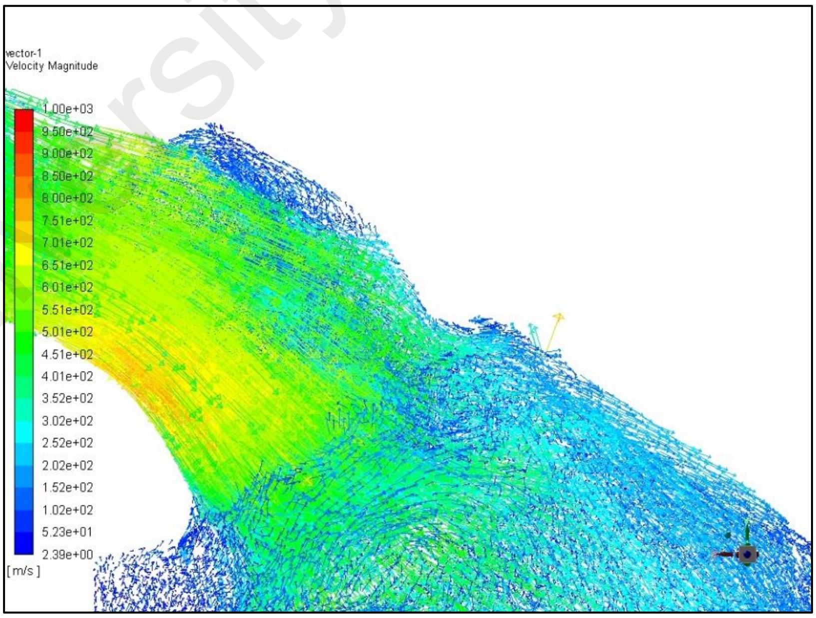

Figure 4.26: Fluid Velocity Around the 23 mm Intake Valve at 9 mm Lift

Figure 4.26 shows fluid velocity entering the combustion chamber through the intake valve. At 9 mm valve opening, the fluid velocity around the valve opening is varies

between 2.02 x 10^2 m/s to 3.0 x 10^2 m/s. However, at this lift value, the small area with high velocity profile nearby valve seat is completely vanished.

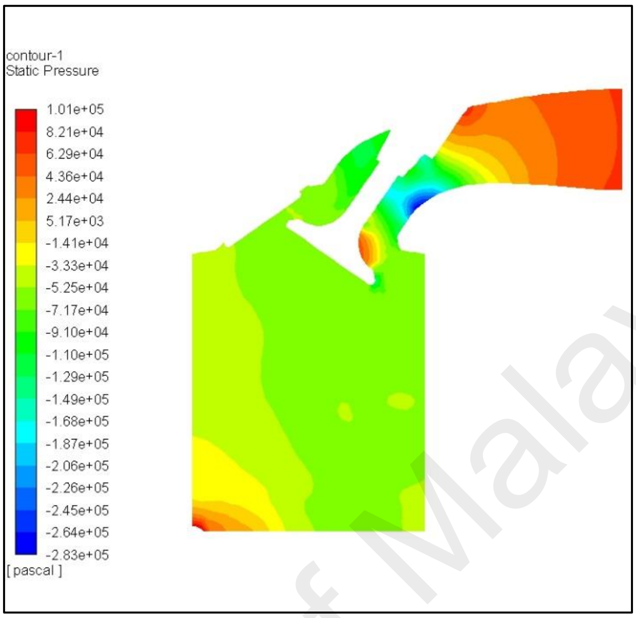

Figure 4.27:Pressure Contour of 23 mm Intake Valve Lift at 9 mm Lift

Figure 4.27 shows the pressure contour of the cylinder during the 9 mm valve opening. At this point, it is found that most of the cylinder pressure is between -7.17x 10^4 Pa to -5.25 x 10^4 Pa.

4.2 Result for 27 mm Intake Valve Diameter

In this chapter, the results of the simulation of valve lifts opening from 1 mm to 9 mm for valve 27 mm diameter intake valve size will be presented.

4.2.1 1 mm Valve Lift Height

Figure 4.28 shows the velocity results of the simulation for the 1mm valve lift. The focus will be on the fluid velocity around the intake valve located in the combustion chamber section as the Figure 4.29.

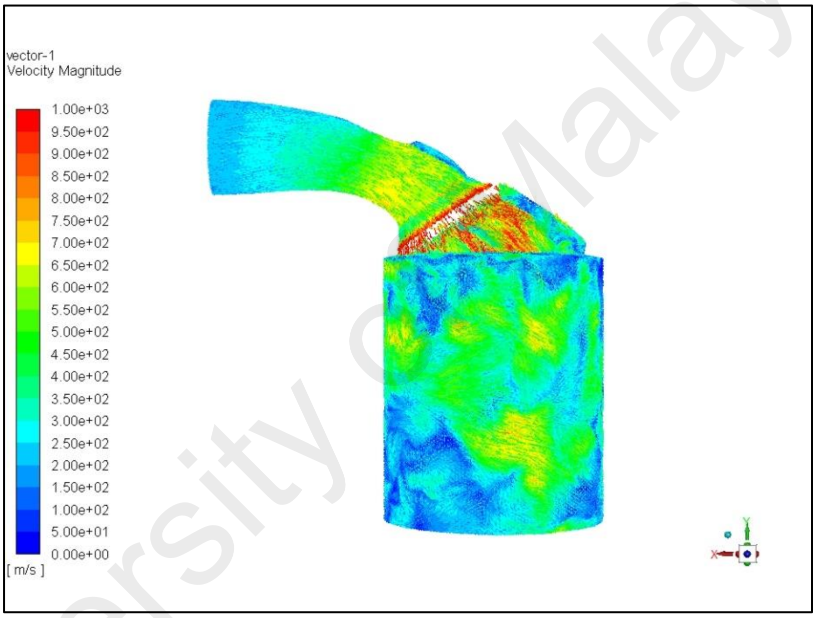

Figure 4.28: Velocity Profile of 27 mm Intake Valve at 1 mm Lift

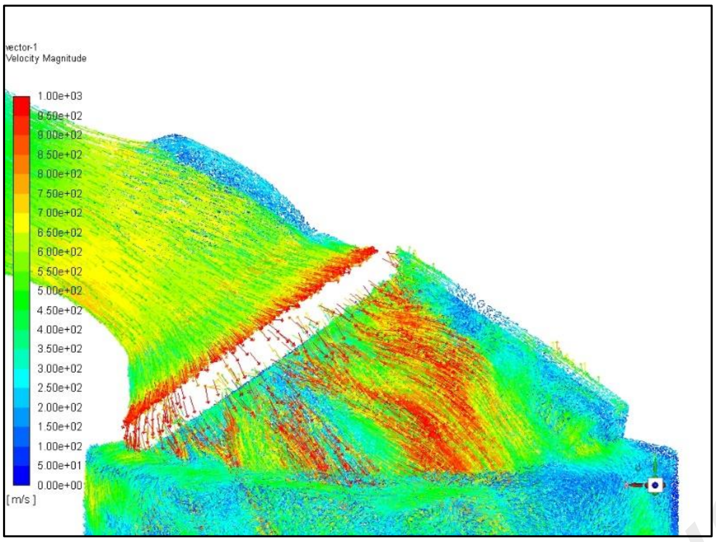

Figure 4.29: Fluid Velocity Around the 27 mm Intake Valve at 1 mm Lift

Figure 4.29 shows fluid velocity entering the combustion chamber through the 27 mm intake valve opening. At 1mm valve lift, the fluid velocity around the valve opening is at a large range between 5 x 10^1 m/s to 1x 10^3 m/s.

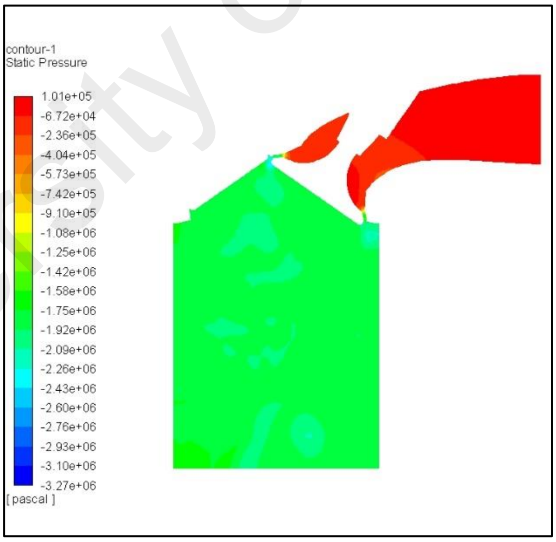

Figure 4.30: Pressure Contour of 27 mm Intake Valve Lift at 1 mm Lift

Figure 4.30 shows the pressure contour of the cylinder during the 1 mm valve lift. At this point, it is found that most of the cylinder pressure is between -2.09x 10^6 Pa to -1.92 x 10^6 Pa.

4.2.2 2 mm Valve Lift Height

Figure 4.31 shows the velocity results of the simulation for the 27 mm intake valve at 2 mm valve lift.

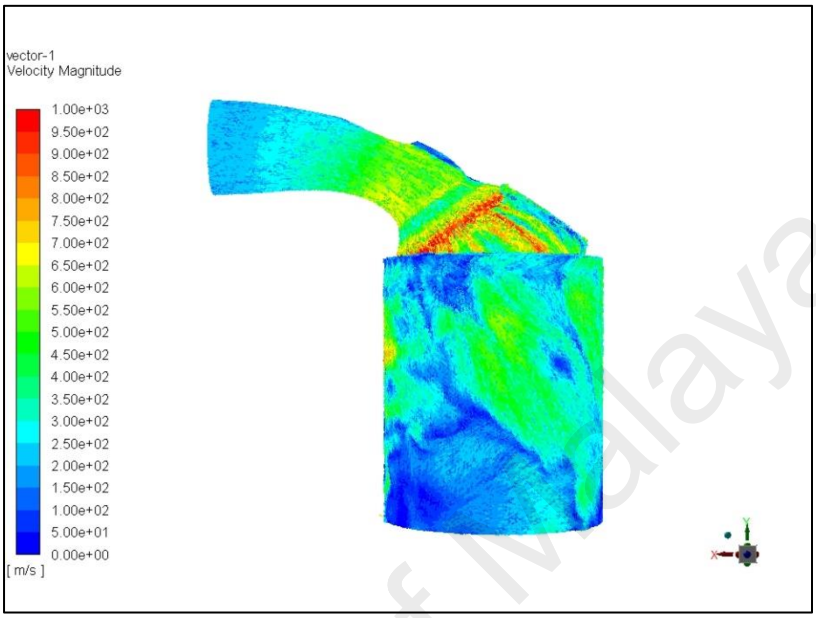

Figure 4.31: Velocity Profile of 27 mm Intake Valve at 2 mm Lift

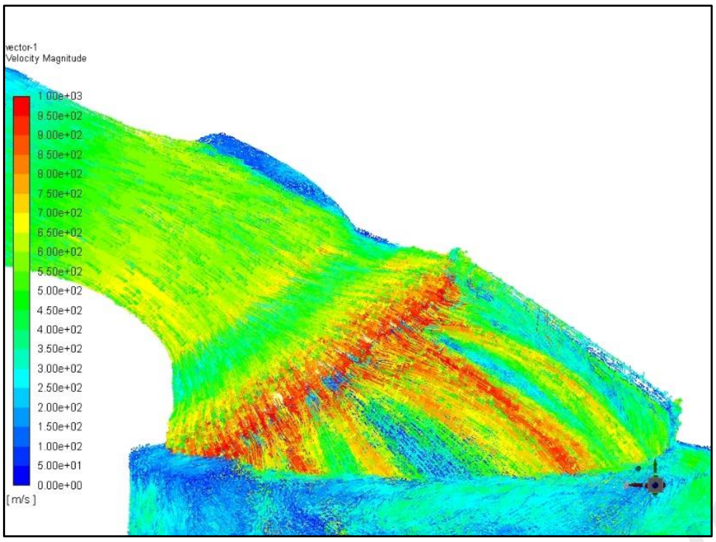

Figure 4.32: Fluid Velocity Around the 27 mm Intake Valve at 2 mm Lift

Figure 4.32 shows fluid velocity entering the combustion chamber through the 27 mm intake valve opening. At 2 mm valve lift, the fluid velocity around the valve opening is at a large range between 5 x 10^1 m/s to 1x 10^3 m/s.

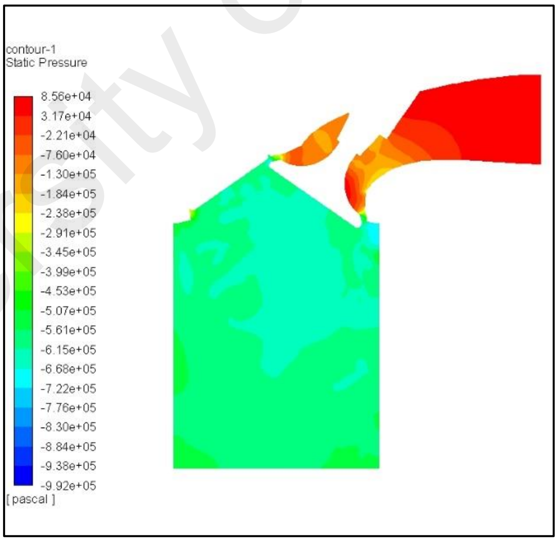

Figure 4.33: Pressure Contour of 27 mm Intake Valve Lift at 2 mm Lift

Figure 4.33 shows the pressure contour of the cylinder during the 1 mm valve lift. At this point, it is found that most of the cylinder pressure is between -6.68x 10^5 Pa to -5.61 x 10^5 Pa.

4.2.3 3 mm Valve Lift Height

Figure 4.34 shows the velocity results of the simulation for the 27 mm intake valve at 3 mm valve lift.

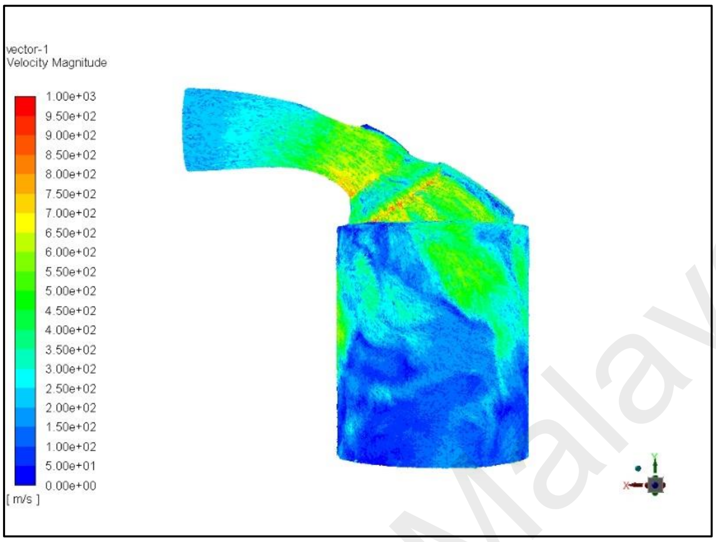

Figure 4.34: Velocity Profile of 27 mm Intake Valve at 3 mm Lift

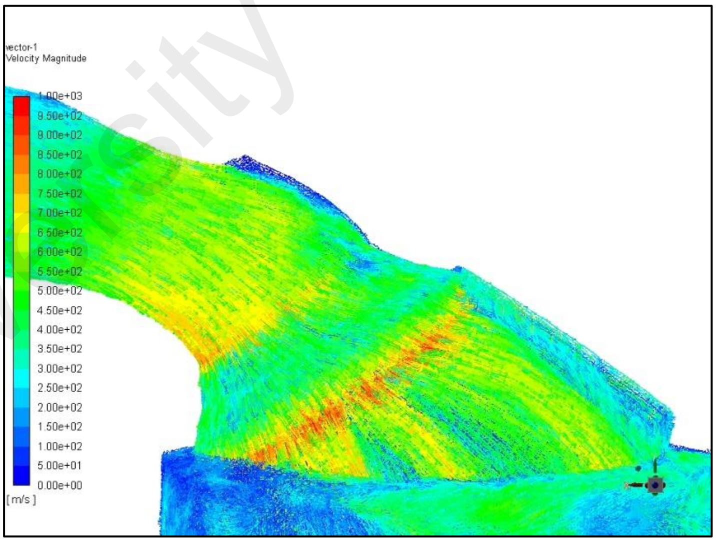

Figure 4.35: Fluid Velocity Around the 27 mm Intake Valve at 3 mm Lift

Figure 4.35 shows fluid velocity entering the combustion chamber through the 27 mm intake valve opening. At 3 mm valve lift, the fluid velocity around the valve opening is at a large range between 5×10^1 m/s to 9×10^2 m/s.

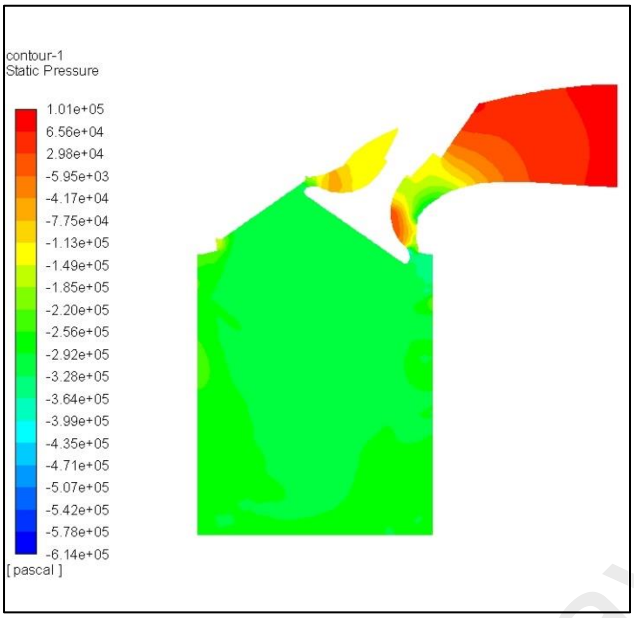

Figure 4.36: Pressure Contour of 27 mm Intake Valve Lift at 3 mm Lift

Figure 4.36 shows the pressure contour of the cylinder during the 3 mm valve lift. At this point, it is found that most of the cylinder pressure is between -2.92x 10^5 Pa to -2.56 x 10^5 Pa.

4.2.4 4 mm Valve Lift Height

Figure 4.37 shows the velocity results of the simulation for the 27 mm intake valve at 4 mm valve lift.

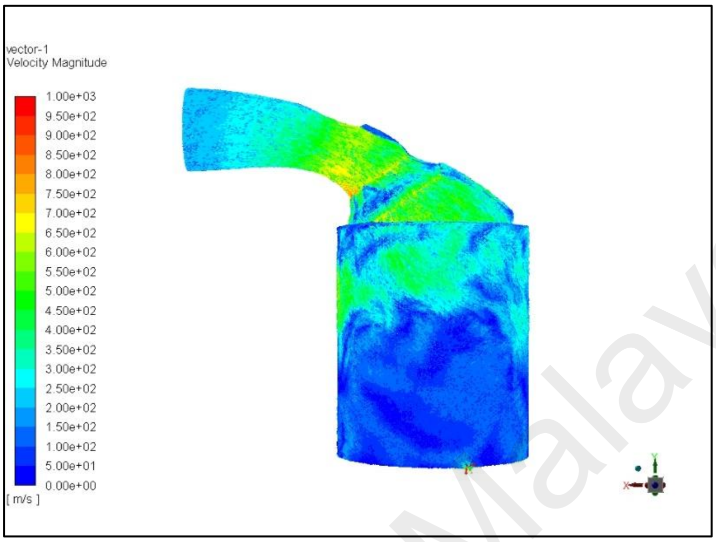

Figure 4.37: Velocity Profile of 27 mm Intake Valve at 4 mm Lift

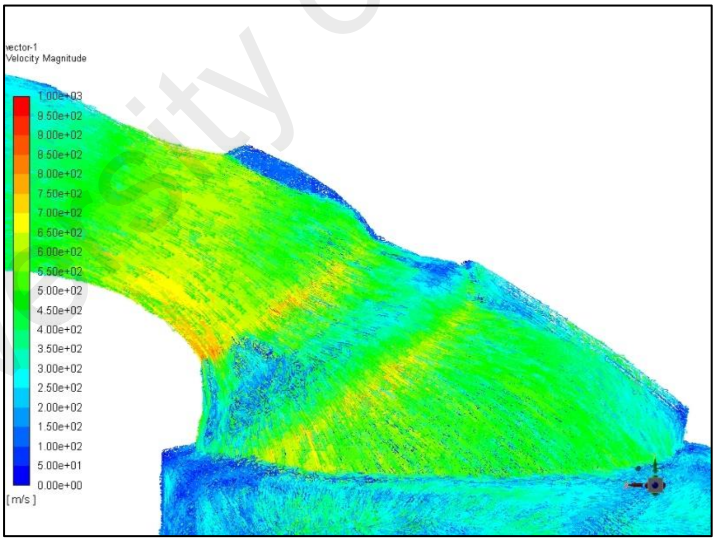

Figure 4.38: Fluid Velocity Around the 27 mm Intake Valve at 4 mm Lift

Figure 4.38 shows fluid velocity entering the combustion chamber through the 27 mm intake valve opening. At 4 mm valve lift, the fluid velocity around the valve opening is at a range between 5 x 10^1 m/s to 6x 10^2 m/s.

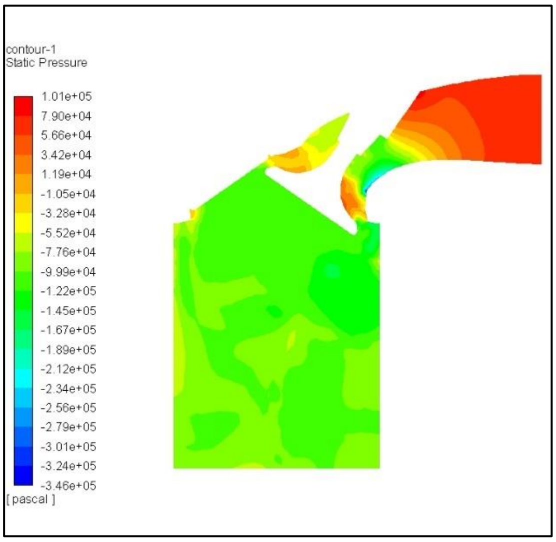

Figure 4.39: Pressure Contour of 27 mm Intake Valve Lift at 4 mm Lift

Figure 4.39 shows the pressure contour of the cylinder during the 4 mm valve lift. At this point, it is found that most of the cylinder pressure is between -9.99x 10^4 Pa to -7.76 x 10^4 Pa.

4.2.5 5 mm Valve Lift Height

Figure 4.40 shows the velocity results of the simulation for the 27 mm intake valve at 5 mm valve lift.

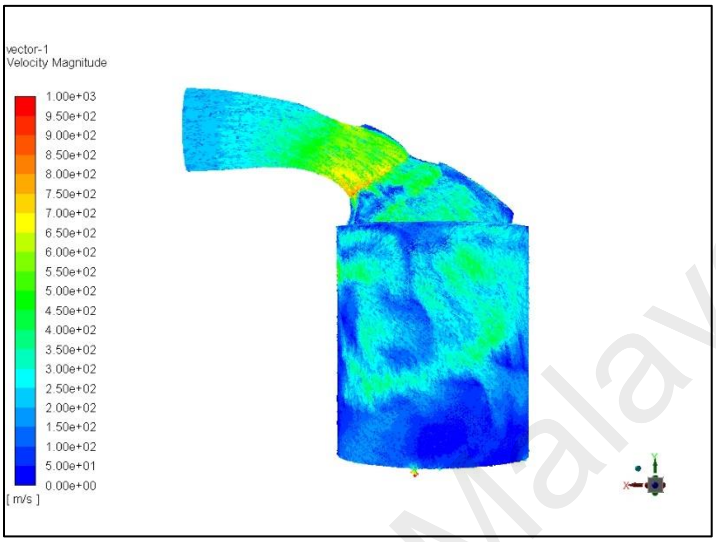

Figure 4.40: Velocity Profile of 27 mm Intake Valve at 5 mm Lift

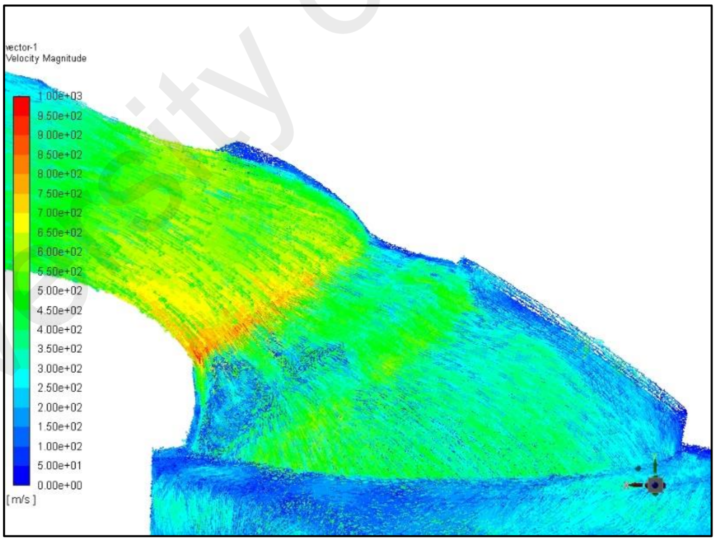

Figure 4.41: Fluid Velocity Around the 27 mm Intake Valve at 5 mm Lift

Figure 4.41 shows fluid velocity entering the combustion chamber through the 27 mm intake valve opening. At 5 mm valve lift, the fluid velocity around the valve opening is at a range between 5 x 10^1 m/s to 4.5x 10^2 m/s.

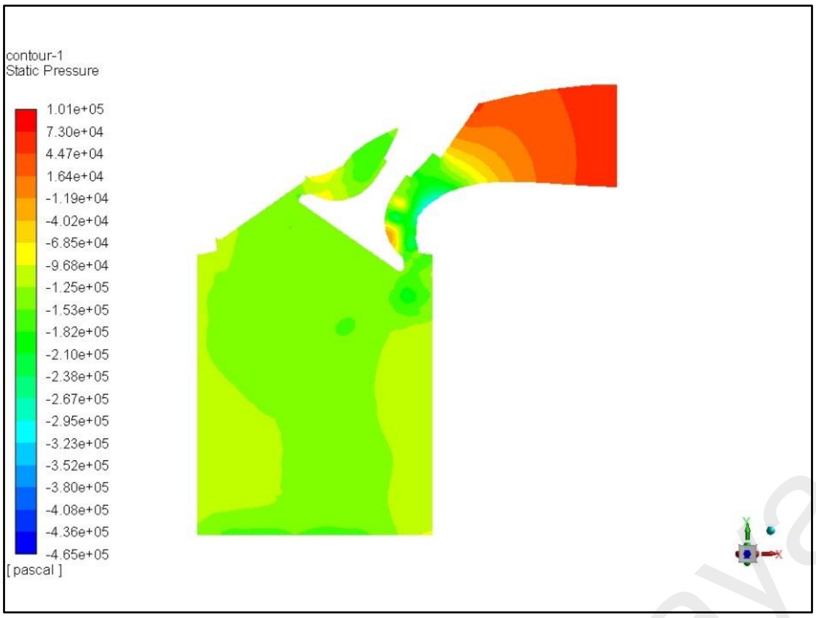

Figure 4.42: Pressure Contour of 27 mm Intake Valve Lift at 5 mm Lift

Figure 4.42 shows the pressure contour of the cylinder during the 5 mm valve lift. At this point, it is found that most of the cylinder pressure is between -1.53x 10^5 Pa to -9.68 x 10^4 Pa.

4.2.6 6 mm Valve Lift Height

Figure 4.43 shows the velocity results of the simulation for the 27 mm intake valve at 6 mm valve lift.

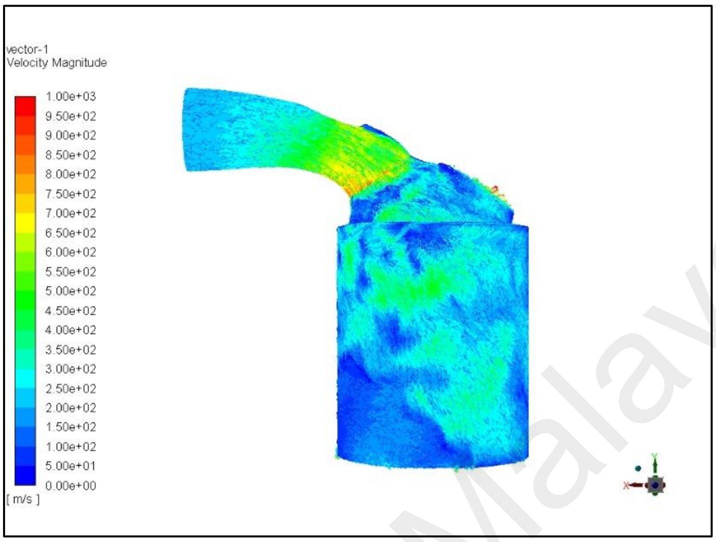

Figure 4.43: Velocity Profile of 27 mm Intake Valve at 6 mm Lift

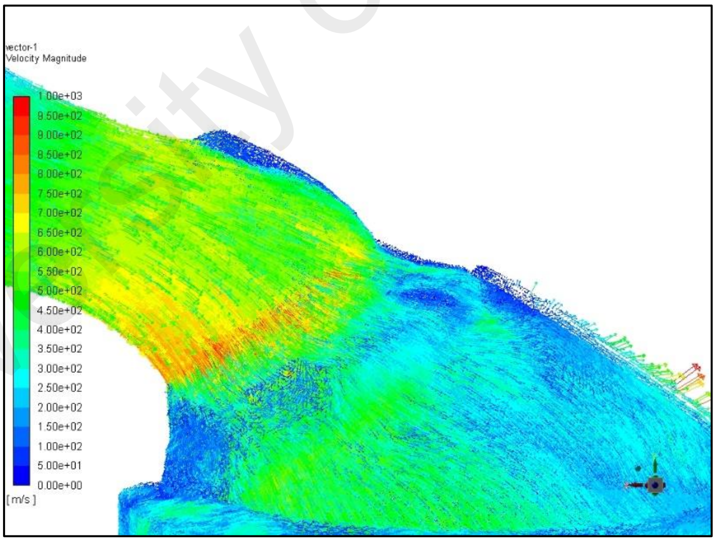

Figure 4.44: Fluid Velocity Around the 27 mm Intake Valve at 6 mm Lift

Figure 4.44 shows fluid velocity entering the combustion chamber through the 27 mm intake valve opening. At 6 mm valve lift, the fluid velocity around the valve opening is at a range between 1 x 10^2 m/s to 5.0x 10^2 m/s.

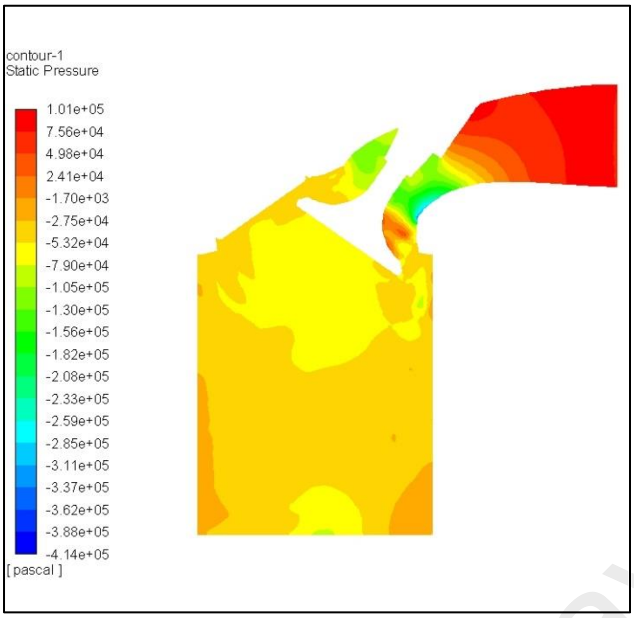

Figure 4.45: Pressure Contour of 27 mm Intake Valve Lift at 6 mm Lift

Figure 4.45 shows the pressure contour of the cylinder during the 6 mm valve lift. At this point, it is found that most of the cylinder pressure is between -7.90x 10^4 Pa to -5.32 x 10^4 Pa.

4.2.7 7 mm Valve Lift Height

Figure 4.46 shows the velocity results of the simulation for the 27 mm intake valve at 7 mm valve lift.

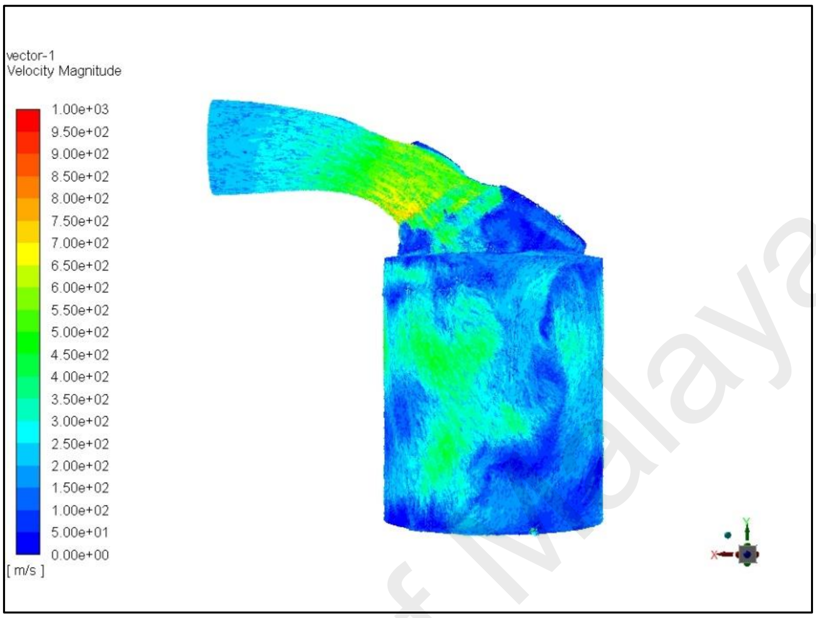

Figure 4.46: Velocity Profile of 27 mm Intake Valve at 7 mm Lift

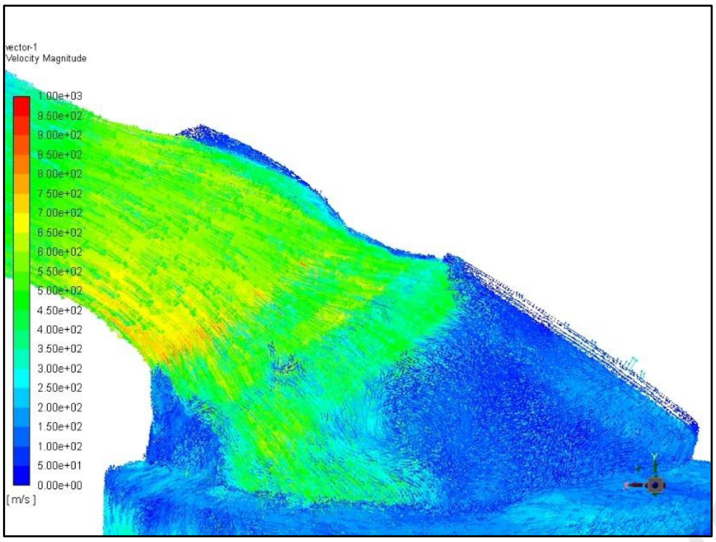

Figure 4.47: Fluid Velocity Around the 27 mm Intake Valve at 7 mm Lift

Figure 4.47 shows fluid velocity entering the combustion chamber through the 27 mm intake valve opening. At 7 mm valve lift, the fluid velocity around the valve opening is at a range between 1.5 x 10^2 m/s to 5.0x 10^2 m/s.

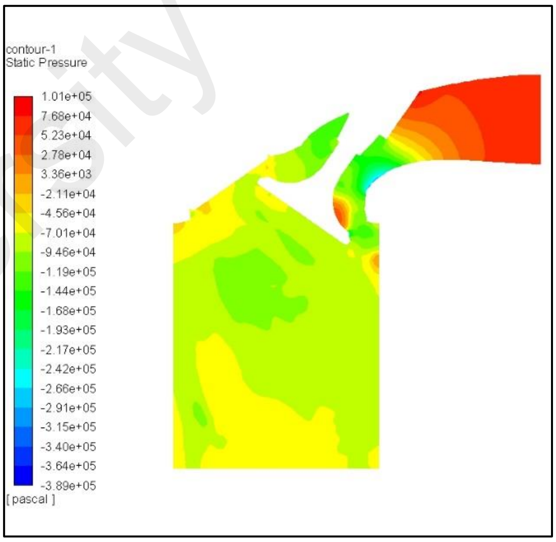

Figure 4.48: Pressure Contour of 27 mm Intake Valve Lift at 7 mm Lift

Figure 4.48 shows the pressure contour of the cylinder during the 7 mm valve lift. At this point, it is found that most of the cylinder pressure is between -9.46x 10^5 Pa to -7.01 x 10^4 Pa.

4.2.8 8 mm Valve Lift Height

Figure 4.49 shows the velocity results of the simulation for the 27 mm intake valve at 8 mm valve lift.

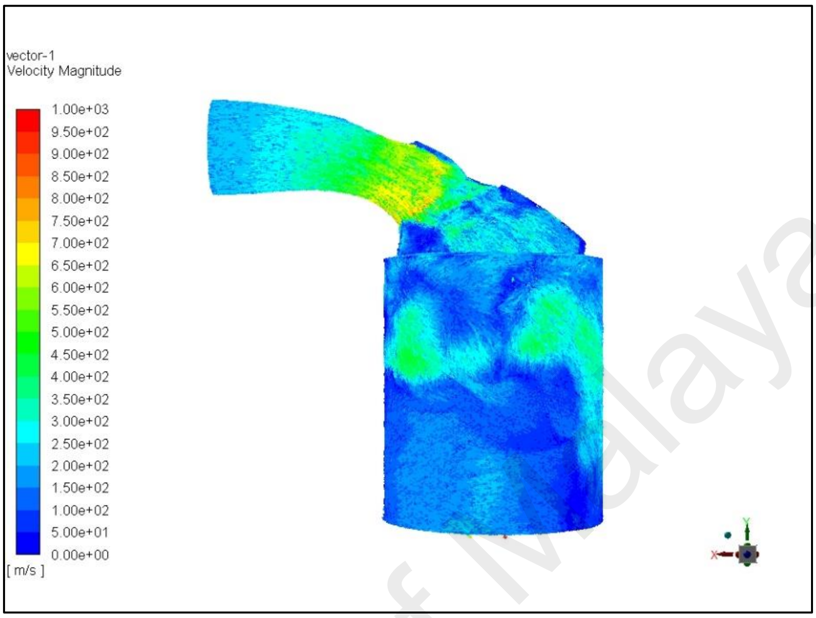

Figure 4.49: Velocity Profile of 27 mm Intake Valve at 8 mm Lift

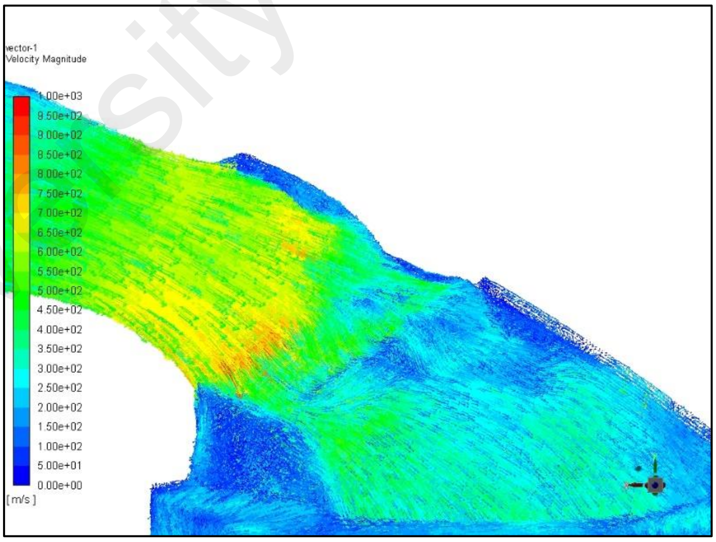

Figure 4.50: Fluid Velocity Around the 27 mm Intake Valve at 8 mm Lift

Figure 4.50 shows fluid velocity entering the combustion chamber through the 27 mm intake valve opening. At 8 mm valve lift, the fluid velocity around the valve opening is at a range between 1.5 x 10^2 m/s to 3.5x 10^2 m/s.

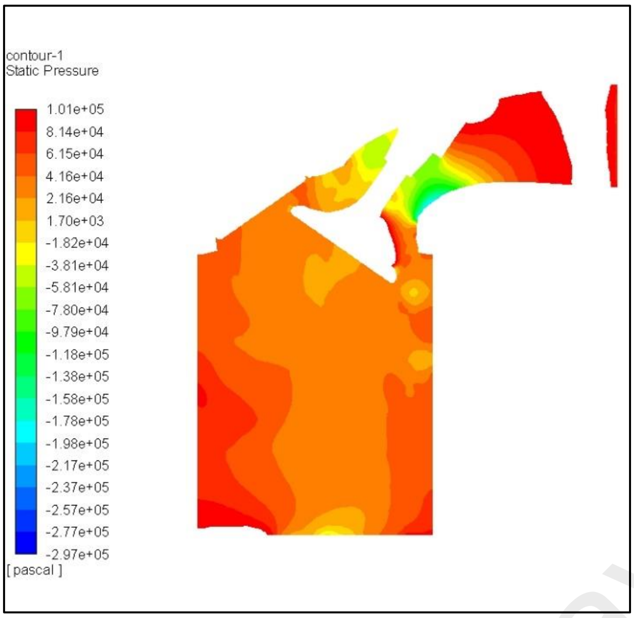

Figure 4.51: Pressure Contour of 27 mm Intake Valve Lift at 8 mm Lift

Figure 4.51 shows the pressure contour of the cylinder during the 8 mm valve lift. At this point, it is found that most of the cylinder pressure is between -1.82 x 10^4 Pa to 1.70 x 10^3 Pa

4.2.9 9 mm Valve Lift Height

Figure 4.52 shows the velocity results of the simulation for the 27 mm intake valve at 9 mm valve lift.

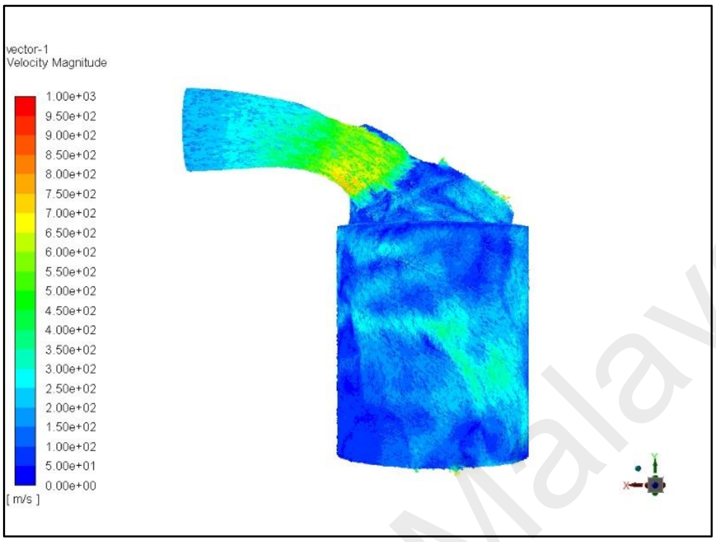

Figure 4.52: Velocity Profile of 27 mm Intake Valve at 9 mm Lift

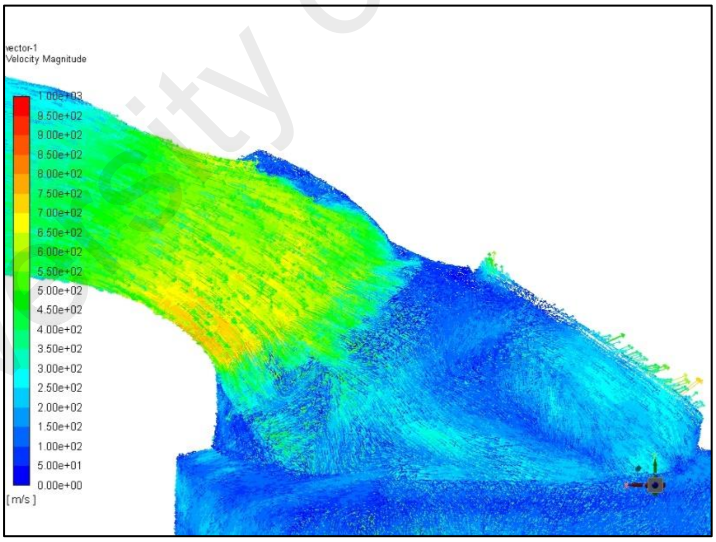

Figure 4.53: Fluid Velocity Around the 27 mm Intake Valve at 9 mm Lift

Figure 4.53 shows fluid velocity entering the combustion chamber through the 27 mm intake valve opening. At 9 mm valve lift, the fluid velocity around the valve opening is at a range between 1.5 x 10^2 m/s to 3.0x 10^2 m/s.

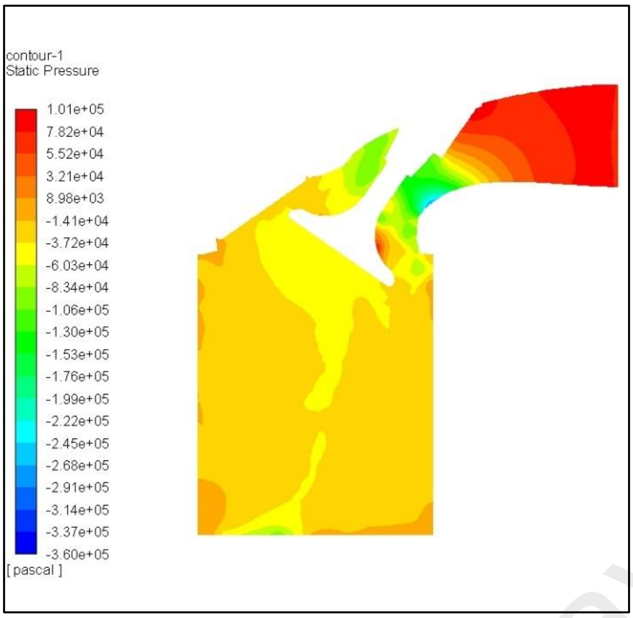

Figure 4.54: Pressure Contour of 27 mm Intake Valve Lift at 9 mm Lift

Figure 4.54 shows the pressure contour of the cylinder during the 8 mm valve lift. At this point, it is found that most of the cylinder pressure is between -6.03 x 10^4 Pa to -3.72 x 10^4 Pa

CHAPTER 5: DISCUSSION

Simulation results obtained have been analyzed to study the velocity and pressure pattern for each valve height profile. In this chapter, the comparison of velocity changes that occurs when the valve lift changes from 1 mm to 9 mm will be made. The comparison of pressure changes in the cylinder will also be presented during the valve lift change.

5.1 23 mm Intake Valve Diameter

5.1.1 Velocity Vector of 23 mm Intake Valve Diameter

Figure 5.1 shows the simulation results for the 23 mm intake valve diameter. The velocity profile for each valve lift height profile will be analyzed further in the next paragraph.

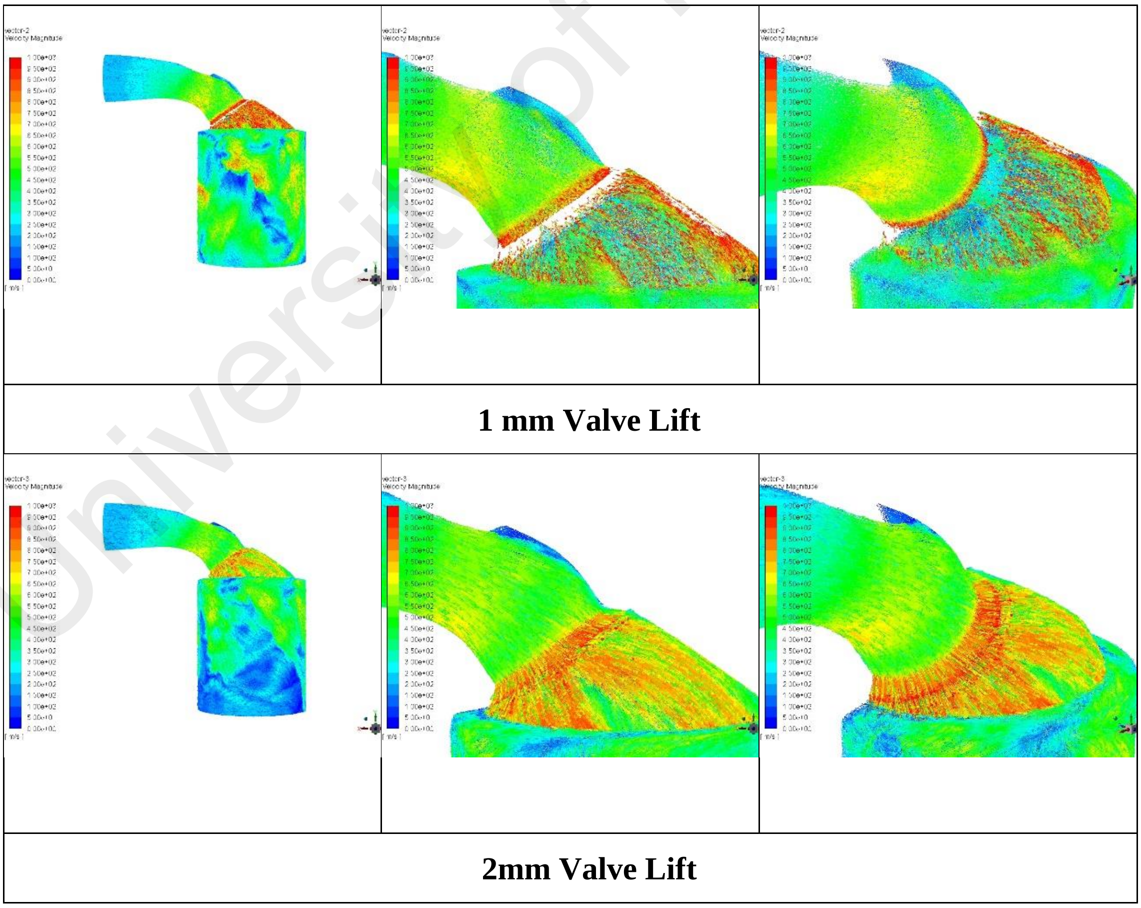

Figure 5.1: Velocity Vector of 23 mm Intake Valve Diameter

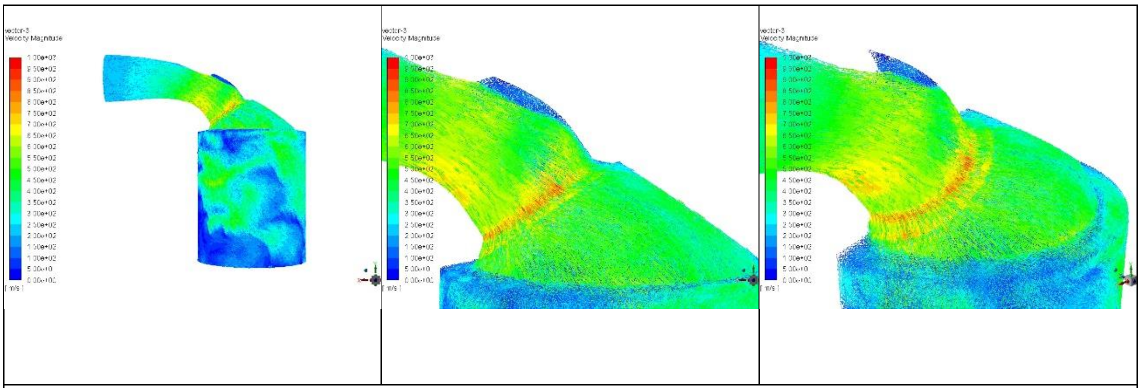

3mm Valve Lift

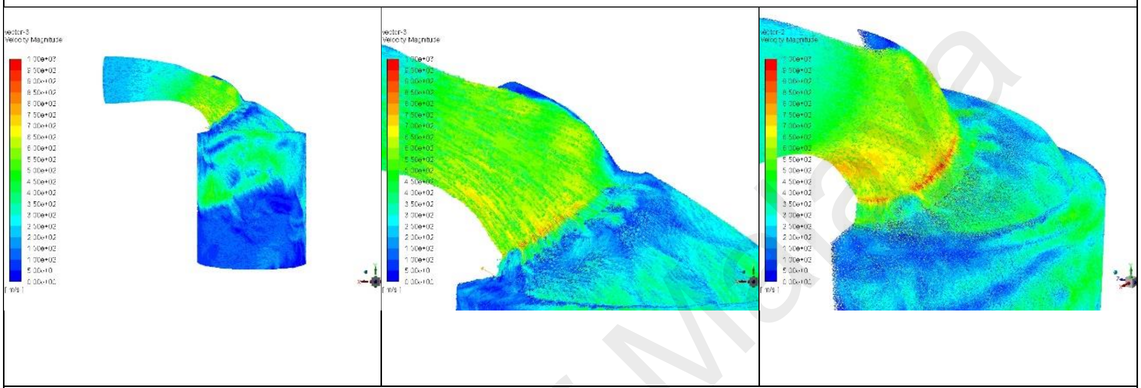

4mm Valve Lift

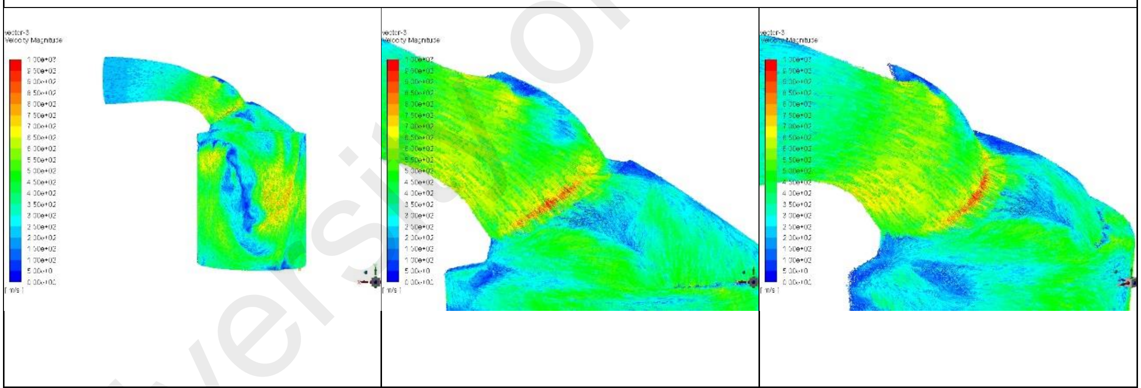

5mm Valve Lift

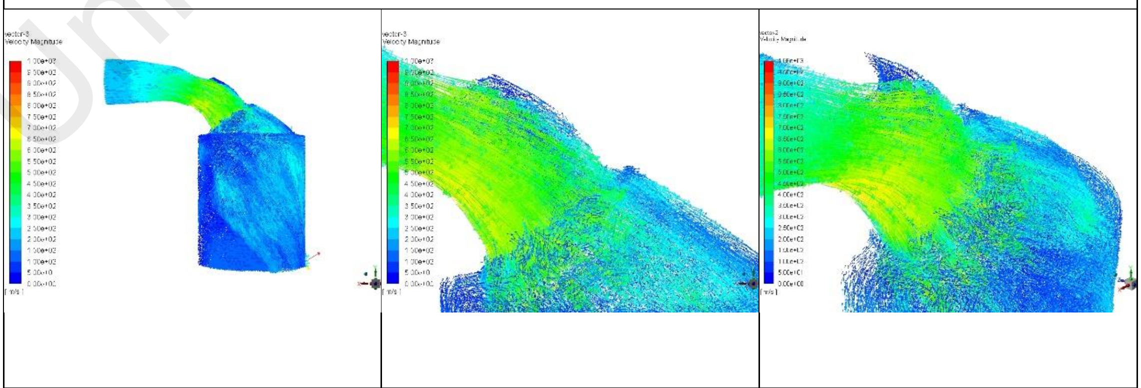

6mm Valve Lift

Figure 5.1: Velocity Vector of 23 mm Intake Valve Diameter (continued)

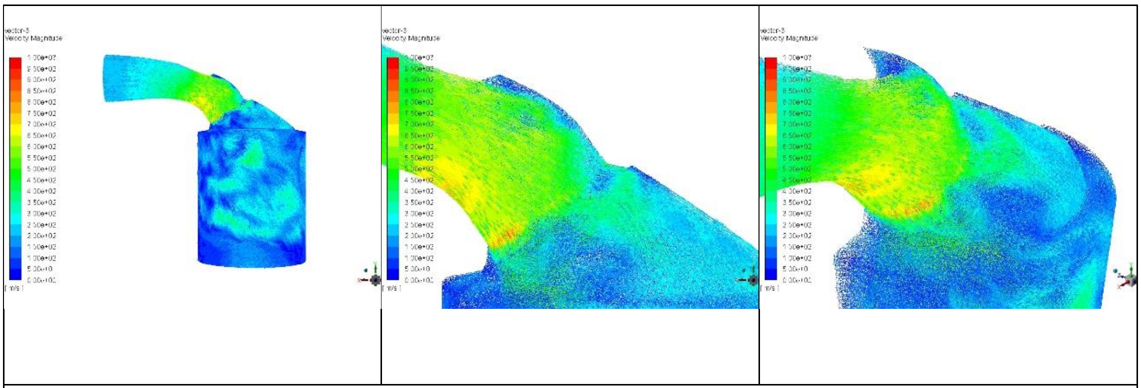

7mm Valve Lift

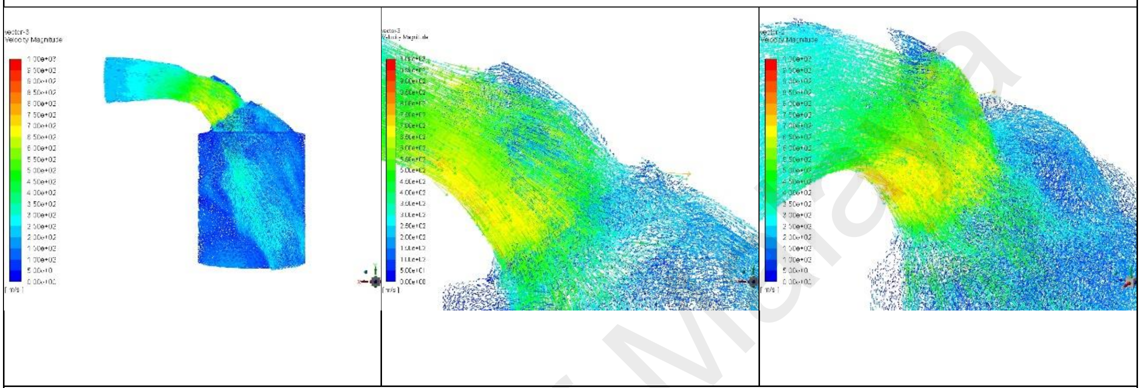

8mm Valve Lift

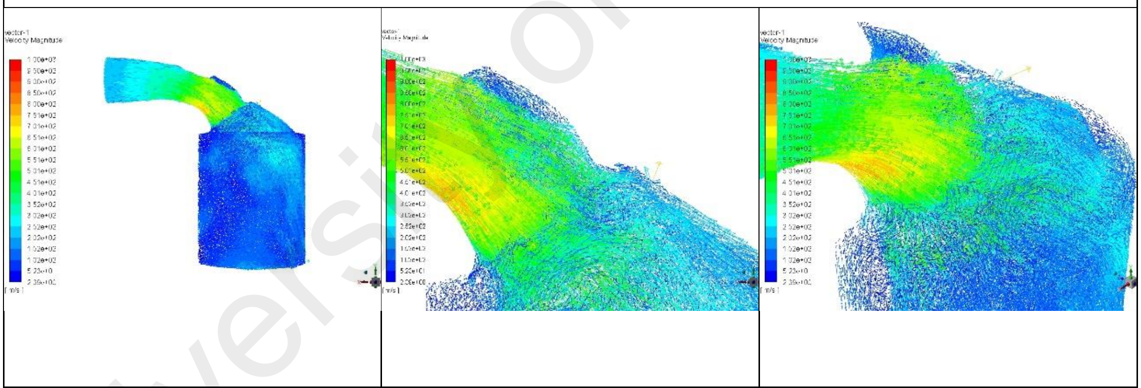

9mm Valve Lift

Figure 5.1: Velocity Profile of 23 mm Intake Valve Diameter (continued)

The simulation results for 1mm up to 5mm valve height indicate the fluid around the intake valve opening has a velocity mixed from low velocity to high velocity. This condition can be seen in a variety of mixed colors that represent the fluid velocity in the valve openings. At 1mm valve opening, there are many red high velocities particles. When the openings increase, the presence of this high velocity particle is decreasing. Fluid velocity is also seen increasingly evenly between one another. When the valve opening reaches 6mm, the presence of red high velocity particles aroung intake valve opening has completely disappeared. Fluid velocity at valve openings is seen more uniformly from one another. This condition is constant and unchanged for higher valve openings for 6 mm, 7 mm, 8mm and 9mm.

5.1.2 Pressure Contours of 23 mm Intake Valve Diameter

Figure 5.2 shows pressure contours results for 23 mm intake valve simulation. Further analysis was conducted to study the changes in pressure that occurred from the intake chamber and the combustion chamber.

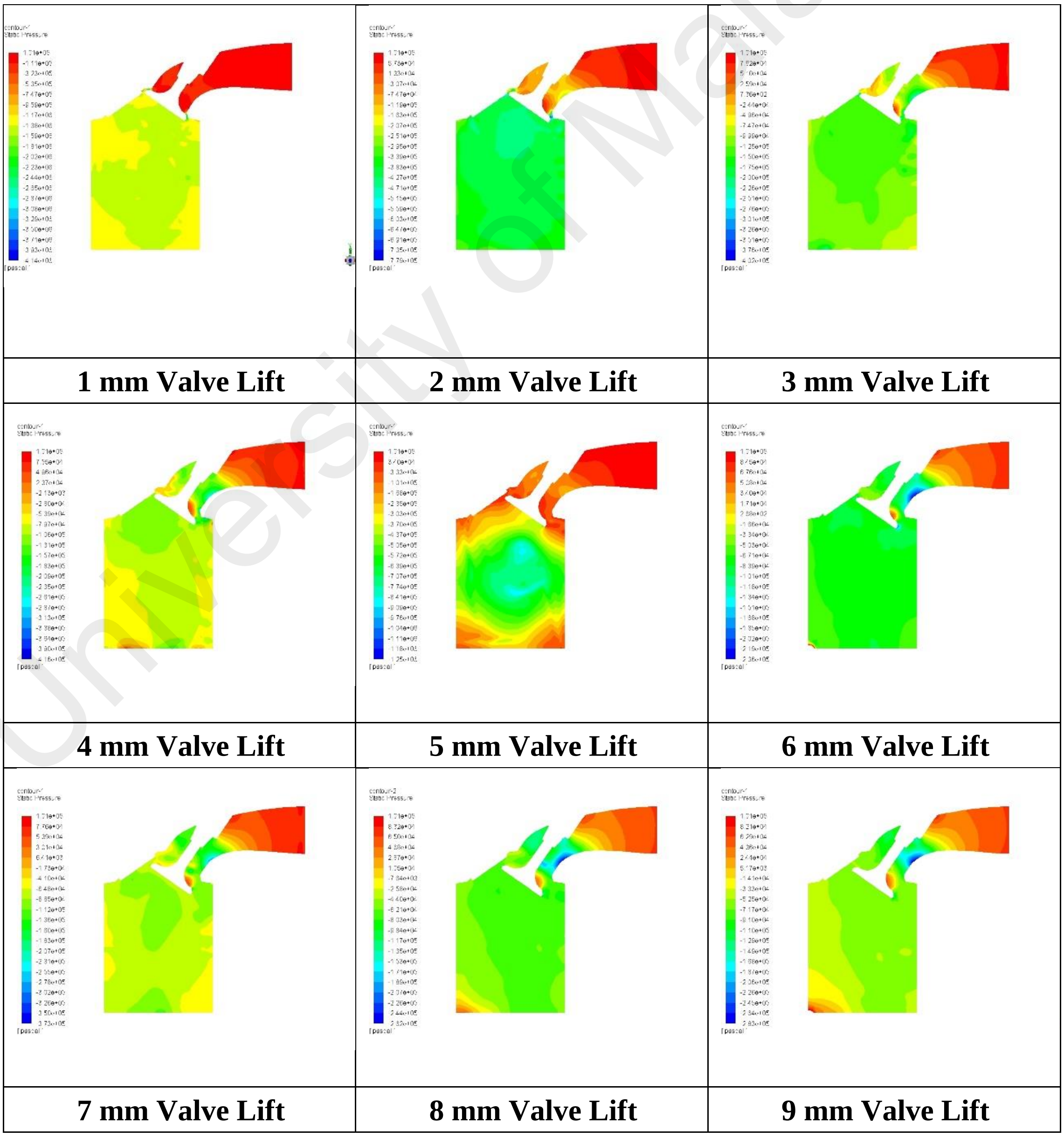

Figure 5.2: Pressure Contour of 23 mm Intake Valve Diameter

Table 5.1 shows the value of the pressure within the combustion chamber. From the data, it is found that the pressure value is negative on all valve lift values. 1mm valve lift shows the lowest pressure value. When the valve opening increases between 1mm to 5mm, the pressure in the combustion increases significantly. But the intangible change pattern can be observed when the valve opening is between 6mm and 9mm. In this range, it is found that the increase in valve lift does not significantly increase the combustion chamber pressure.

Table 5.1: Combustion Chamber Pressure of 23 mm Intake Valve Diameter

Valve Lift (mm)	Combustion Chamber Pressure (kPa)
1	-1380
2	-471
3	-175
4	-106
5	-205
6	-67.1
7	-64.8
8	-62.1
9	-52.5

From the Figure 5.3, at the openings of 1mm valve up to 5mm, the pressure change in engine cylinder is very significant. It is found that at the valve lift range of 6mm to 9mm, it is found that the pressure change pattern is horizontal and has no significant difference.

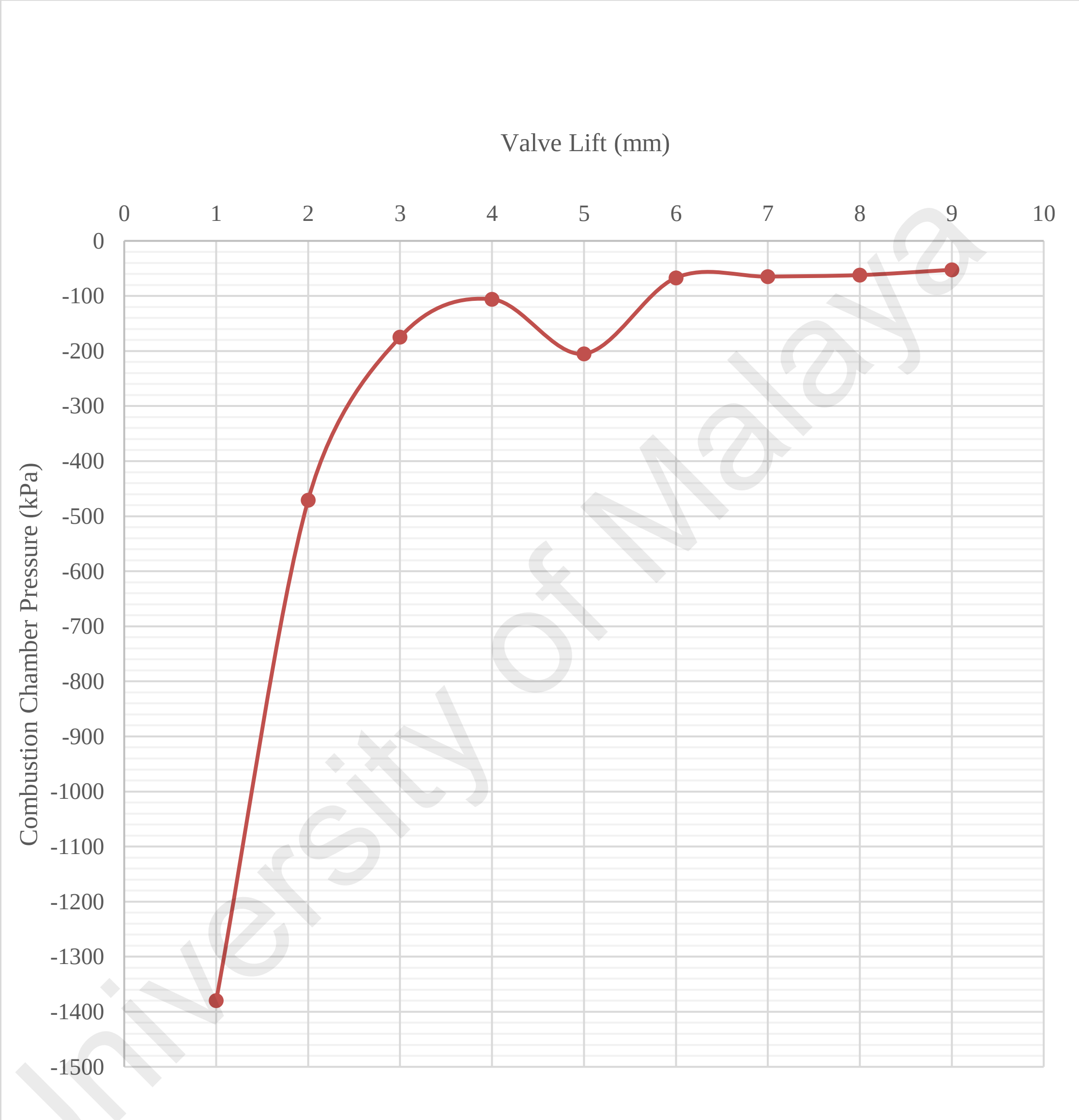

Figure 5.3: Combustion Chamber Pressure Pattern of 23mm Intake Valve Diameter

5.2 27 mm Intake Valve Diameter

5.2.1 Velocity Vector for 27 mm Intake Valve Diameter

Figure 5.4 shows the simulation results for the 27mm intake valve diameter. The velocity profile for each valve lift height profile will be analyzed further in the next paragraph.

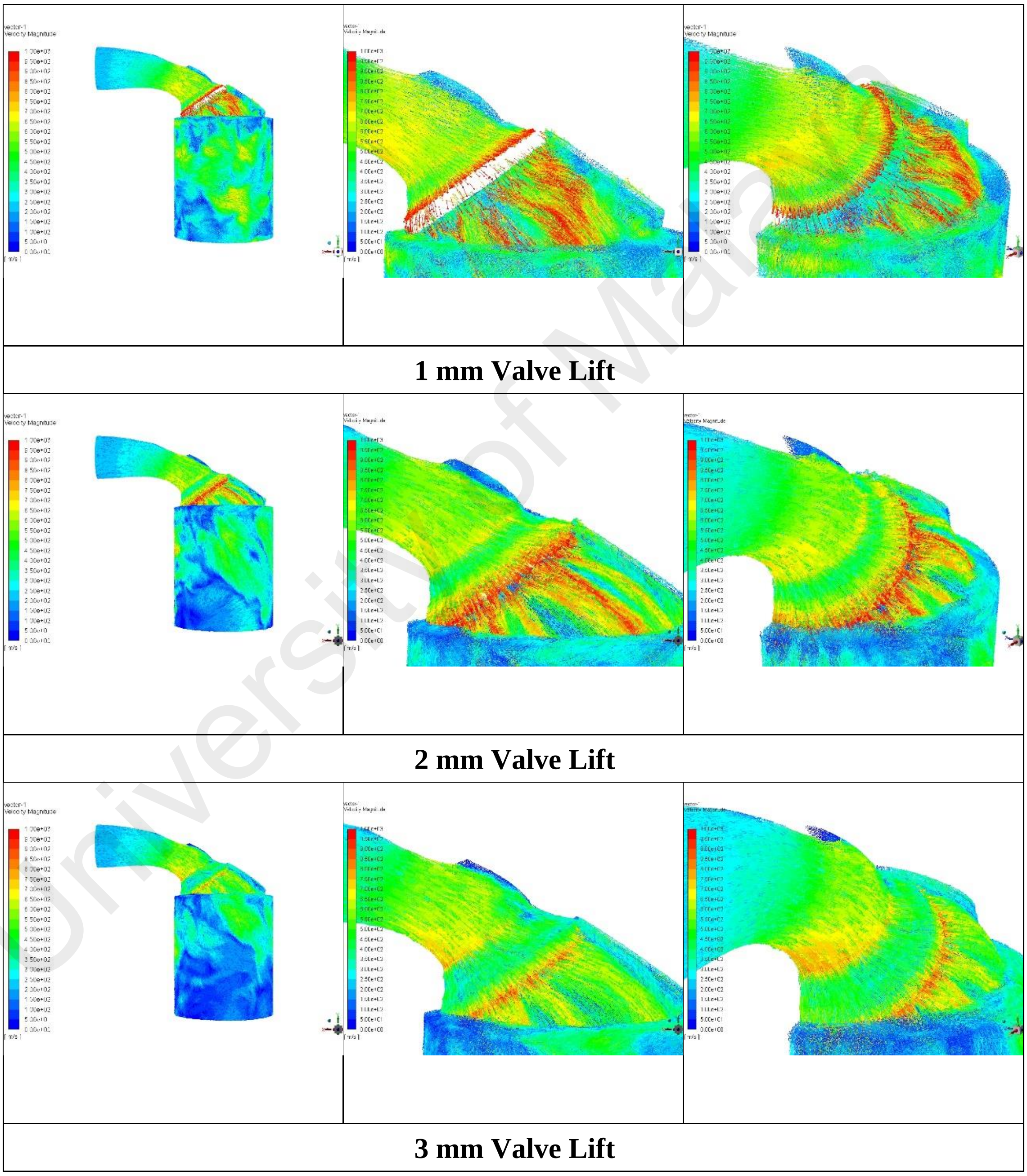

Figure 5.4: Velocity Vector of 27 mm Intake Valve Diameter

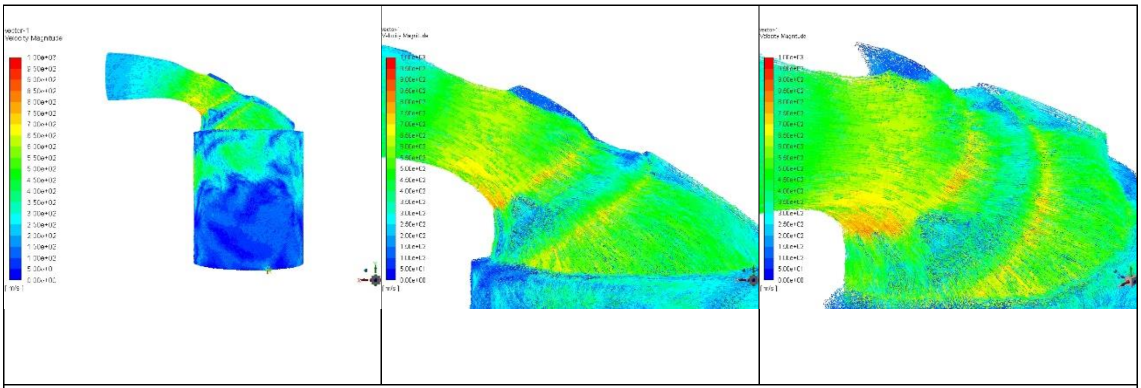

4 mm Valve Lift

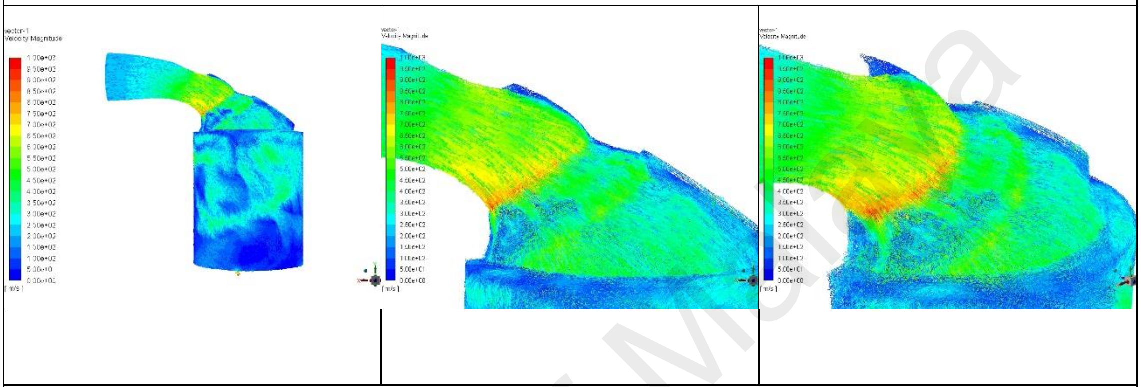

5 mm Valve Lift

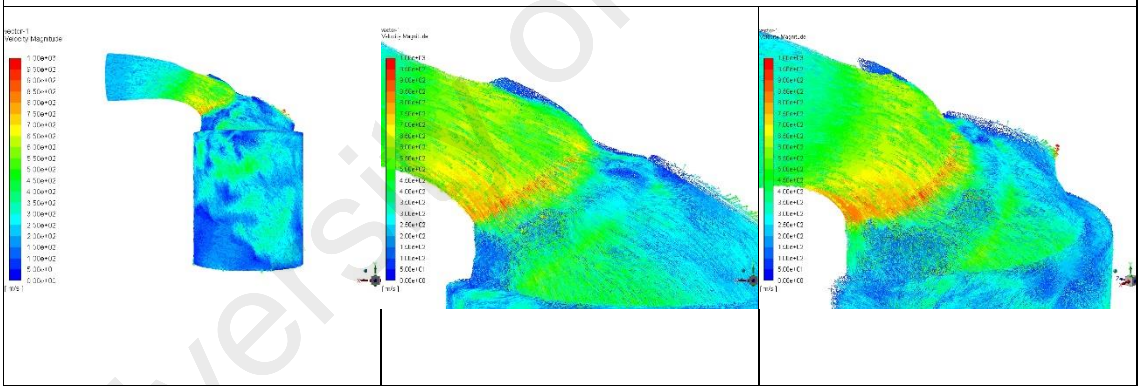

6 mm Valve Lift

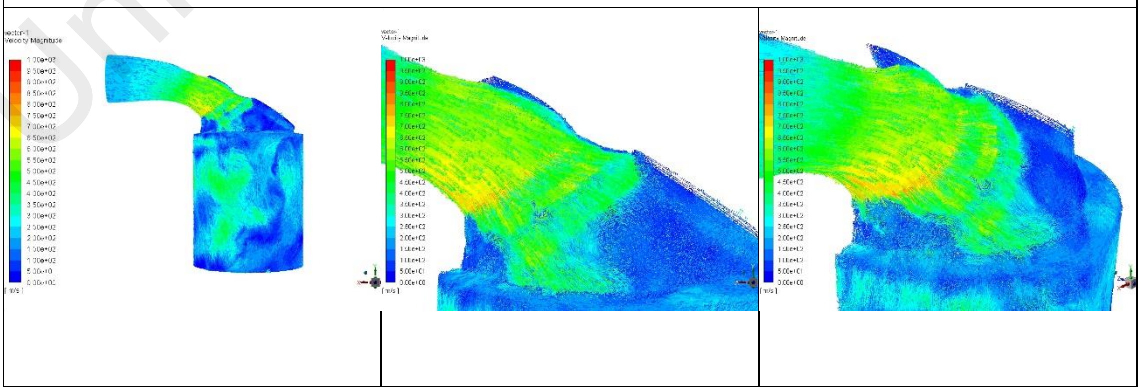

7 mm Valve Lift

Figure 5.4: Velocity Profile of 27 mm Intake Valve Diameter (continued)

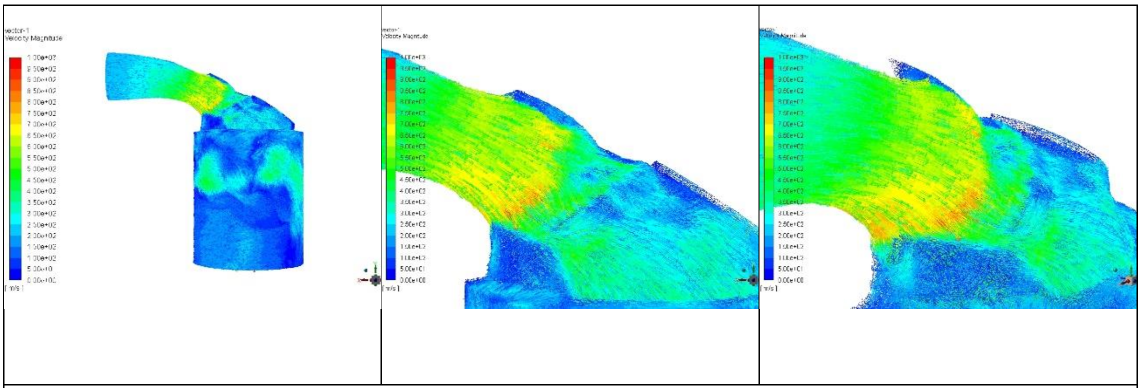

8 mm Valve Lift

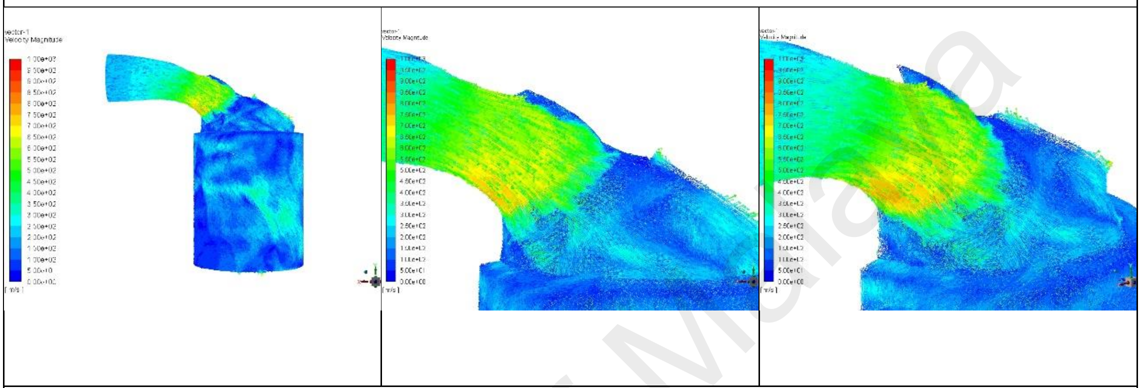

9 mm Valve Lift

Figure 5.4: Velocity Vector of 27 mm Intake Valve Diameter (continued)

The simulation results for 1mm up to 3mm valve height indicate the fluid around the intake valve opening has a velocity mixed from low velocity to high velocity. This condition can be seen in a variety of mixed colors that represent the fluid velocity in the valve openings. At 1mm valve opening, there are many red high velocities particles. When the openings increase, the presence of this high velocity particle is decreasing. Fluid velocity is also seen increasingly evenly between one another. When the valve opening reaches 4mm, the presence of red high velocity particles has completely disappeared. Fluid velocity at valve openings is seen more uniformly from one another. This condition is constant and unchanged for higher valve openings for 4 mm, 5 mm, 6 mm, 7 mm, 8 mm and 9 mm.

5.2.2 Pressure Contours for 27 mm Intake Valve Diameter

Figure 5.5 shows pressure contours results for 27 mm intake valve simulation. Further analysis was conducted to study the changes in pressure that occurred from the intake chamber and the combustion chamber.

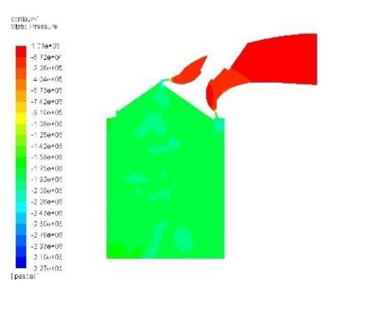	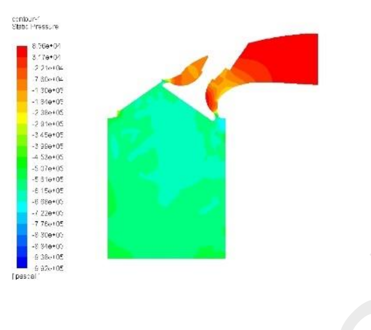	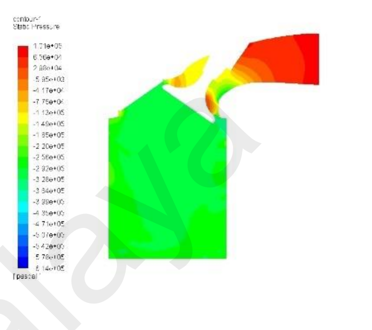
1 mm Valve Lift	**2 mm Valve Lift**	**3 mm Valve Lift**
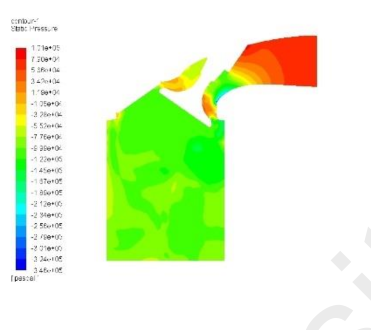	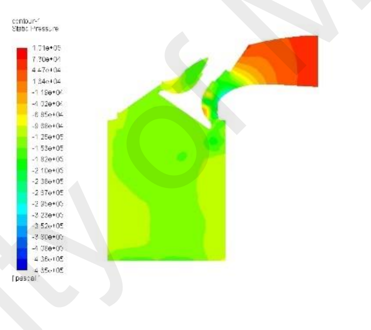	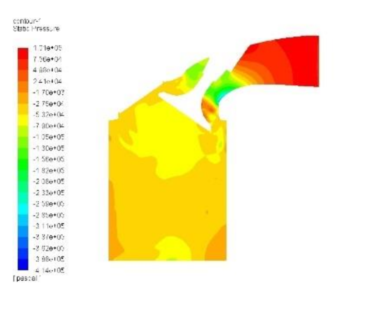
4 mm Valve Lift	**5 mm Valve Lift**	**6 mm Valve Lift**
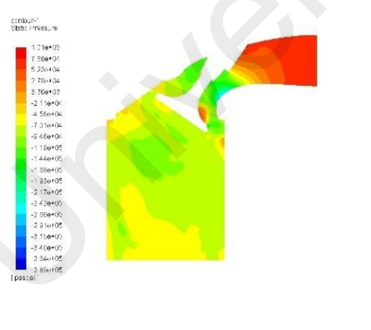	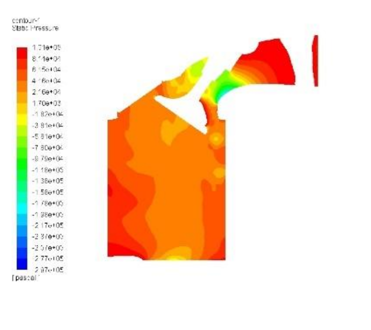	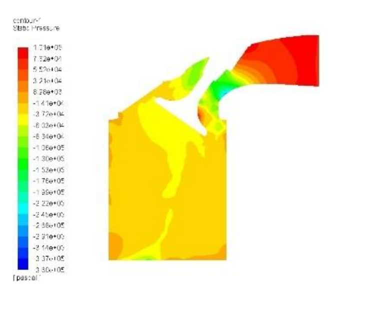
7 mm Valve Lift	**8 mm Valve Lift**	**9 mm Valve Lift**

Figure 5.5: Pressure Contour of 27 mm Intake Valve Diameter

Table 5.2 shows the value of the pressure within the combustion chamber. From the data, it is found that the pressure value is negative on all valve lift values. 1mm valve lift shows the lowest pressure value. When the valve opening increases between 1mm to 3mm, the pressure in the combustion increases significantly. But the intangible change pattern can be observed when the valve opening is between 4mm and 9mm. In this range, it is found that the increase in valve lift does not significantly increase the combustion chamber pressure.

Table 5.2: Combustion Chamber Pressure of 27 mm Intake Valve Diameter

Valve Lift (mm)	Combustion Chamber Pressure (kPa)
1	-1420
2	-615
3	-292
4	-99.9
5	-96.8
6	-79
7	-70.1
8	-64.1
9	-60.3

From the Figure 5.6, at the openings of 1mm valve up to 3mm, the pressure change in engine cylinder is very significant. It is found that at the valve lift range of 4mm to 9mm, the pressure change pattern is horizontal and has no significant difference.

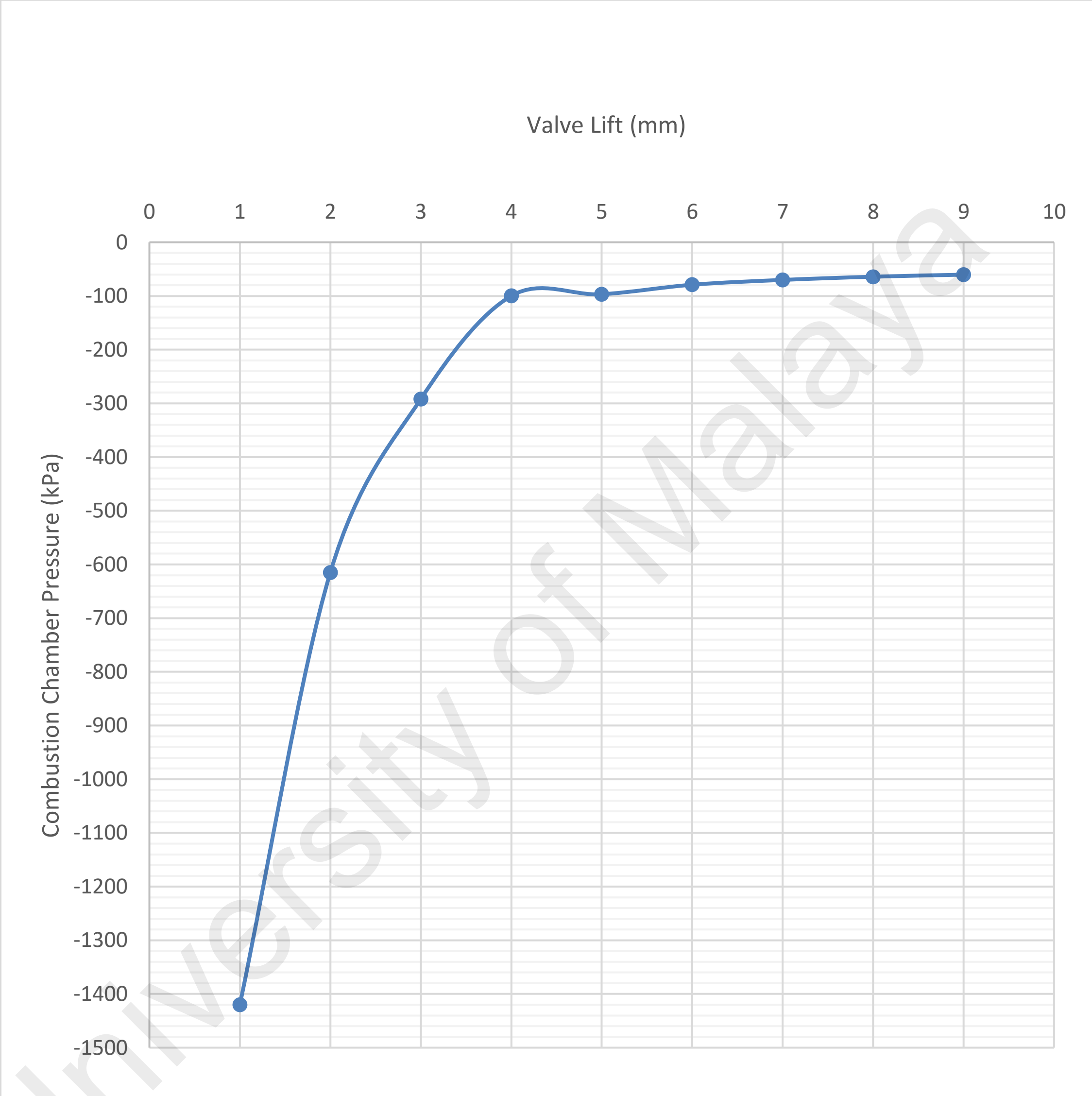

Figure 5.6: Combustion Chamber Pressure Pattern of 27mm Intake Valve Diameter

CHAPTER 6: CONCLUSION

The research project that has been carried out has met the desired objectives. Through the results obtained, it is found that the valve lift affects the velocity of the fluid into the engine combustion chamber. Through an air pressure analysis, it is found that the valve lift value also affects the pressure inside the engine cylinder. However, the study also found that cylinder pressure was also heavily influenced by the valve lift value. When exceeding the optimum valve lift height, it is found that the pressure in the cylinder has no significant change even though the height of the valve lift is increased

From the computational fluid dynamic simulations, result and analysis carried out, it was found that, for a 23 mm diameter valve size, the optimum valve lift required was 6 mm. Valve lifts lower than 6 mm will restrict fluid entrance into the combustion chamber. However, increasing the valve lift exceeds the 6mm value does not significantly increase the amount of fluid entering into the engine cylinder during the intake stroke of four (4) cycle gasoline engine.

For a 27 mm diameter valve size, the optimum valve lift required was 4 mm. Valve lifts lower than 4 mm will restrict fluid entrance into the combustion chamber. However, increasing the valve lift exceeds the 4mm value does not significantly increase the amount of fluid entering into the engine cylinder during the intake stroke of four (4) cycle gasoline engine.

REFERENCES

Antonelli, M., Baccioli, A., Francesconi, M., & Martorano, L. (2014). Experimental and Numerical Analysis of the Valve Timing Effects on the Performances of a Small Volumetric Rotary Expansion Device. *Energy Procedia, 45*, 1077-1086.

Bong, K. F. (2011). *Investigation of Flow Around a Golf Driver Head Using CFD*: Jabatan Kejuruteraan Rekabentuk dan Pembuatan, Fakulti Kejuruteraan, Universiti Malaya.

Blanco, H. P. (2004). Experimental characterization of mass, work and heat flows in an air cooled, single cylinder engine. *Energy Conversion and Management, 45*, 157–169.

Brusiani, F., Falfari, S., & Cazzoli, G. (2014). Tumble Motion Generation in Small Gasoline Engines: A New Methodological Approach for the Analysis of the Influence of the Intake Duct Geometrical Parameters. *Energy Procedia, 45*, 997-1006.

Catellani, C., Cazzoli, G., Falfari, S., Forte, C., & Bianchi, G. M. (2016). Large Eddy Simulation of a Steady Flow Test Bench Using OpenFOAM®. *Energy Procedia, 101*, 622-629.

Celik, I., Yavuz, I., & Smirnov, A. (2001). Large eddy simulations of in-cylinder turbulence for internal combustion engines: A review. *International Journal of Engine Research, 2*(2), 119-148. doi:10.1243/1468087011545389

Çinar, C., Şahin, F., Can, Ö., & Uyumaz, A. (2016). A comparison of performance and exhaust emissions with different valve lift profiles between gasoline and LPG fuels in a SI engine. *Applied Thermal Engineering, 107*(Supplement C), 1261-1268.

Cinar, C., Uyumaz, A., Solmaz, H., & Topgul, T. (2015). Effects of valve lift on the combustion and emissions of a HCCI gasoline engine. *Energy Conversion and Management, 94*(Supplement C), 159-168.

Claudio, F., Cristian, C., Giulio, C., Marco, B. G., Stefania, F., Federico, B., . . . Stefano, S. (2015). Numerical Evaluation of the Applicability of Steady Test Bench Swirl Ratios to Diesel Engine Dynamic Conditions. *Energy Procedia, 81*, 732-741.

Clenci, A. C., Iorga-Simăn, V., Deligant, M., Podevin, P., Descombes, G., & Niculescu, R. (2014). A CFD (computational fluid dynamics) study on the effects of operating an engine with low intake valve lift at idle corresponding speed. *Energy, 71*(Supplement C), 202-217.

Dalla Nora, M., Lanzanova, T. D. M., & Zhao, H. (2016). Effects of valve timing, valve lift and exhaust backpressure on performance and gas exchanging of a two-stroke GDI engine with overhead valves. *Energy Conversion and Management, 123*(Supplement C), 71-83.

Detroit. (2018). MBE 4000 VALVES. Retrieved from http://www.detroitmanuals.info/mbe-4000/0A0213.html

Dovat, F. (2018). What is the difference between the Atkinson and Otto cycles? Why is the Atkinson engine used in hybrid cars? Retrieved from https://www.quora.com/What-is-the-difference-between-the-Atkinson-and-Otto-cycles-Why-is-the-Atkinson-engine-used-in-hybrid-cars-1

Falfari, S., Brusiani, F., & Bianchi, G. M. (2014). Numerical Analysis of In-cylinder Tumble Flow Structures – Parametric 0D Model Development. *Energy Procedia, 45*, 987-996.

Falfari, S., Brusiani, F., & Pelloni, P. (2014). 3D CFD Analysis of the Influence of Some Geometrical Engine Parameters on Small PFI Engine Performances – the Effects on the Tumble Motion and the Mean Turbulent Intensity Distribution. *Energy Procedia, 45*(Supplement C), 701-710.

Fontana, G., & Galloni, E. (2009). Variable valve timing for fuel economy improvement in a small spark-ignition engine. *Applied Energy, 86*(1), 96-105.

Forte, C., Bianchi, G. M., Corti, E., Fantoni, S., & Costa, M. (2014). CFD Methodology for the Evaluation of Knock of a PFI Twin Spark Engine. *Energy Procedia, 45*, 859-868.

Giannakopoulos, G. K., Frouzakis, C. E., Boulouchos, K., Fischer, P. F., & Tomboulides, A. G. (2017). Direct numerical simulation of the flow in the intake pipe of an internal combustion engine. *International Journal of Heat and Fluid Flow, 68*(Supplement C), 257-268.

Heywood, J. B. (1988). Internal combustion engine fundamentals.

Hong, H., Parvate-Patil, G. B., & Gordon, B. (2004). Review and analysis of variable valve timing strategies—eight ways to approach. *Proceedings of the Institution of Mechanical Engineers, Part D: Journal of Automobile Engineering, 218*(10), 1179-1200.

Jia, M., Xie, M., Wang, T., & Peng, Z. (2011). The effect of injection timing and intake valve close timing on performance and emissions of diesel PCCI engine with a full engine cycle CFD simulation. *Applied Energy, 88*(9), 2967-2975.

Li, Y., Khajepour, A., Devaud, C., & Liu, K. (2017). Power and fuel economy optimizations of gasoline engines using hydraulic variable valve actuation system. *Applied Energy, 206*, 577-593.

Lubken, J. (2016). Camshaft Specifications and Terminology. Retrieved from https://www.speedwaymotors.com/the-toolbox/camshaft-specifications-and-terminology/28647

Lunati. (2008). Understanding Camshaft Specifications. Retrieved from http://www.lunatipower.com/Tech/Cams/CamSpecTerms.aspx

McAulay, K., Wu, T., Chen, S. K., Borman, G. L., Myers, P. S., & Uyehara, O. A. (1966). Development and evaluation of the simulation of the compression-ignition engine. *SAE Transactions*, 560-593.

Nigro, A., Algieri, A., De Bartolo, C., & Bova, S. (2017). Fluid dynamic investigation of innovative intake strategies for multivalve internal combustion engines. *International Journal of Mechanical Sciences, 123*(Supplement C), 297-310.

Ravi, M., & Marathe, A. (1992). Effect of port sizes and timings on the scavenging characteristics of a uniflow scavenged engine. *SAE Transactions*, 1571-1589.

Roberpj. (2018). The Role of CFD Analysis in Engine Design. Retrieved from https://www.sharcnet.ca/Software/Ansys/17.0/en-us/help/wb_icom/icom_cfd_role.html

Semlitsch, B., Wang, Y., & Mihăescu, M. (2015). Flow effects due to valve and piston motion in an internal combustion engine exhaust port. *Energy Conversion and Management, 96*(Supplement C), 18-30.

Sridhar, G., Paul, P. J., & Mukunda, H. S. (2004). Simulation of fluid flow in a high compression ratio reciprocating internal combustion engine. *Proceedings of the Institution of Mechanical Engineers, Part A: Journal of Power and Energy, 218*(6), 403-416.

W. Pulkrabek, W. (2004). *Engineering Fundamentals of the Internal Combustion Engine, 2nd Ed* (Vol. 126).

Young, L. (2007). Camshaft Basics and Terminology. Retrieved from https://www.tildentechnologies.com/Cams/CamBasics.html

Yusof, A. S., Ishak, S. A. F. M., Sohaimi, R. M., & Mat, W. A. W. (2016). COMPUTATIONAL SIMULATION AND EXPERIMENTAL VALIDATION OF A TURBOCHARGED DIESEL ENGINE. JURNAL TEKNOLOGI, 78(6-10), 111-116.